




Lifted Schrödinger Bridges for Gaussian Mixture Endpoints: Projection Gaps and Path-Space Obstructions

Siddhartha Ganguly , George Rapakoulias , and Panagiotis Tsiotras 

ABSTRACT. We study stochastic density control between Gaussian-mixture endpoint distributions under Brownian prior dynamics. Since the direct Schrödinger bridge between Gaussian mixtures is generally not available in closed form, we introduce a *lifted path-space construction* in which each trajectory is augmented with a source–target component label. Consequently, the problem decomposes into Gaussian component-to-component Schrödinger bridges with explicit marginal, drift, and cost formulas, while the mixture-level assignment reduces to a finite-dimensional entropic coupling problem with a Sinkhorn scaling form. We then analyze the projection obtained by discarding or forgetting the label. By construction, the projected law satisfies the original Gaussian-mixture endpoint constraints, but its relative entropy generally differs from the lifted relative entropy by a nonnegative conditional label-information gap. This gap reveals a *path-space obstruction*: the lifted optimizer cannot, in general, be identified with the direct unlabeled Schrödinger bridge after projection. We also derive the posterior-averaged Markov drift associated with the projected marginal flow, prove a kinetic-energy upper bound, and identify a common path-potential condition under which the projection gap vanishes. Several numerical illustrations showing density and shape control are recorded for a self-contained exposition.



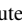
§1. Introduction



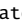


The Schrödinger bridge problem, originally posed by Erwin Schrödinger as a thought experiment [Sch31, Sch32], provides a stochastic counterpart of optimal transport [Vil03, San15, San23]: among all path measures matching two prescribed endpoint distributions, one seeks the most likely evolution relative to a prior stochastic dynamics [Lí4, Pey25, PC20, Föl88]. In the Brownian case, and more generally for diffusion priors, this variational problem is equivalent, through Girsanov’s theorem [KS91, Chapter 3, §3.5], [CGP16, CGP21], to a stochastic optimal control problem with a quadratic control energy cost. This viewpoint has led to a rich set of connections between entropy minimization, optimal transport, stochastic control [PP90, Pra91, MHA26, AEG26, AC24], covariance steering [IK23, Lam25, RPT25], and computational algorithms based on Sinkhorn-type scaling [GKBK24, GZZ24, EMG24, CH21, TWH26].

In parallel, Schrödinger bridge formulations have recently become increasingly visible in modern generative modeling [RH21]. Diffusion and score-based models can be

2020 *Mathematics Subject Classification.* 93E20, 93E03, 49K20, 49L99, 58E25, 65K10.

Key words and phrases. Stochastic optimal control, Schrödinger bridges, optimal transport.

S. Ganguly, G. Rapakoulias, and P. Tsiotras are with  Daniel Guggenheim School of Aerospace,  Georgia Institute of Technology,  Atlanta, USA..

Contact Information: (SG)  <https://sites.google.com/view/siddhartha-ganguly>,  sganguly41@gatech.edu, (GR)  grap@gatech.edu, (PT)  <https://dcs1.gatech.edu/tsiotras.html>,  tsiotras@gatech.edu.

interpreted as stochastic transports [Pey25] between a simple prior distribution and a data distribution. Several recent works formulate or approximate this transport through Schrödinger bridge, entropic optimal transport, score matching, or flow matching perspectives [BTHD21, SSDK⁺21, SBCD23, TMF⁺23, LCBH⁺23, LCST22, LLN⁺24]. For example, diffusion Schrödinger bridge methods connect score-based generative modeling with finite-time entropy-regularized transport, while bridge-matching and simulation-free formulations place diffusion and flow-matching models within a common stochastic transport framework. These developments show that SBs are not only a classical object in stochastic control and optimal transport [DEH26], but also provide a useful mathematical language for generative sampling, data-to-data translation, and learned distributional dynamics.

Despite this general theory, obtaining explicit and computationally viable density-steering laws remains difficult for non-Gaussian endpoint distributions. Gaussian endpoints are, however, special: under Brownian or linear-Gaussian priors, the corresponding Schrödinger bridge remains Gaussian, and its marginal flow, optimal drift, and energy cost admit closed-form or finite-dimensional descriptions [BHCK23, MGM22, CGP18]. Related attempts to analytically verify tractable classes of optimal-transport or transport-type problems beyond the purely Gaussian setting include Gaussian-mixture and Wasserstein-type constructions [CGT18, DD20, RPL⁺26]. However, many density-control and generative-modeling problems of interest are intrinsically multimodal. A natural and expressive model class is given by *Gaussian mixture models*

$$\rho_0 := \sum_{i=1}^{N_1} \alpha_i^0 p_i^0, \quad \rho_1 := \sum_{j=1}^{N_2} \alpha_j^1 p_j^1,$$

where each component p_i^0 and p_j^1 is Gaussian, but the full endpoint densities are generally *non-Gaussian and multimodal*. From the viewpoint of generative modeling, such mixtures provide a simple yet analytically revealing model of multimodal distributions: they retain Gaussian component-wise structure while exhibiting the ambiguity in assigning mass between distinct modes. The direct Schrödinger bridge between such mixtures is not, in general, known to remain within a finite Gaussian-mixture class with closed-form componentwise dynamics. Moreover, the mixture representation introduces a structural ambiguity: the state process itself does not carry the component label and therefore does not specify which initial component should be paired with which terminal component. Thus, while the Gaussian components suggest a tractable decomposition, the original stochastic dynamics remains unlabeled.

This observation motivates the following questions we address in this work:

- (Q-a) Can the Gaussian-mixture structure be exploited without reducing the problem to a purely Gaussian one?
- (Q-b) Can this be achieved by lifting the path space with an auxiliary source–target component label, so that the mixture-to-mixture construction decomposes into tractable Gaussian component-to-component subproblems together with a principled rule for assigning mass between components?
- (Q-c) After solving the resulting lifted, labeled problem on the augmented path space, what precisely is its relationship with the original unlabeled Schrödinger bridge problem on the state path space?
- (Q-d) Can the projected, state-only law be represented by a Markov feedback drift that steers the prescribed Gaussian-mixture endpoints?

These questions brings us to the main conceptual contribution of this manuscript, namely, recast Gaussian-mixture Schrödinger bridge constructions from a lifted path-space

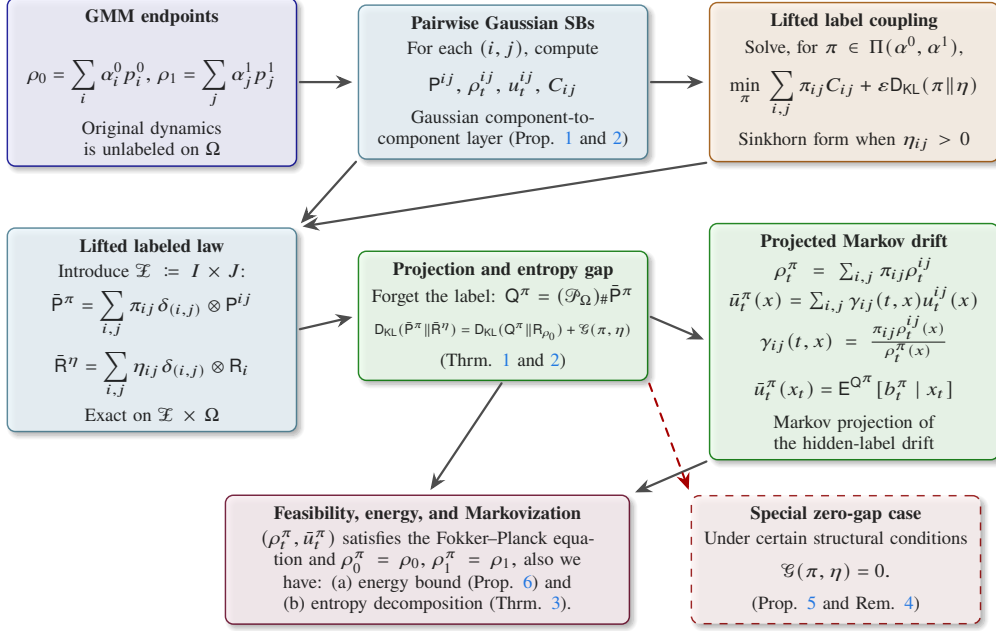


FIGURE 1. Roadmap of our lifted Schrödinger bridge construction.

perspective. Rather than treating a Gaussian-mixture bridge only as a computational superposition of pairwise Gaussian bridges, we formulate an augmented entropy-minimization problem on a label–trajectory space, in which the source–target component assignment is itself a probabilistic object. In this formulation, the prior component coupling η specifies the reference assignment structure in the lifted space, while the optimized coupling π balances this prior assignment against the pairwise Gaussian bridge costs. This viewpoint separates three issues that are often conflated: the exact solution of the lifted labeled problem, the feasibility of its projection onto the original unlabeled path space, and the information gap that prevents the projected law from being identified, in general, with the direct unlabeled Schrödinger bridge. The detailed contributions are as follows (a schematic is given in Figure 1).

- **Lifted formulation for Gaussian-mixture endpoints.** We address (Q-a) by augmenting each trajectory with an auxiliary source–target component label. For a given label (i, j) , the problem becomes a Gaussian Schrödinger bridge from the initial component p_i^0 to the terminal component p_j^1 . Thus, the Gaussian-mixture representation is used as a structural decomposition device. This is an exact construction on the augmented label–trajectory space; it is not, by itself, an assertion that the resulting projected law is the optimizer of the original unlabeled Schrödinger bridge problem.
- **Finite-dimensional entropic assignment of component mass.** We address (Q-b) by showing that, after the pairwise Gaussian bridge costs have been computed, the remaining lifted problem reduces to a finite-dimensional entropic coupling problem over the mixture weights. When the prior coupling η has full support, the optimizer has a Sinkhorn scaling form. This separates the componentwise continuous bridge calculations from the discrete component-assignment problem.
- **Projection gap between the lifted and unlabeled problems.** We address (Q-c) by projecting the lifted law back to the original path space, i.e., by forgetting the auxiliary label. The projected law is feasible for the prescribed Gaussian-mixture endpoints. However, its relative entropy with respect to the original unlabeled Brownian reference generally differs from the lifted relative entropy. We prove a projection identity showing that

the lifted entropy decomposes into the projected path-space entropy plus a nonnegative conditional label-information gap. This gap identifies precisely the obstruction to interpreting the lifted optimizer as the optimizer of the direct unlabeled Schrödinger bridge problem. We also give a structural common path-potential condition under which this projection gap vanishes, showing that the gap is not an unavoidable artifact of lifting.

- **Posterior-averaged Markov density control.** We address (Q-d) by constructing a state-only Markov drift obtained by posterior averaging of the pairwise Gaussian bridge drifts. The resulting density–drift pair satisfies the Fokker–Planck equation, matches the prescribed endpoint densities, and obeys a kinetic-energy upper bound. Posterior-averaged Gaussian-mixture bridge feedback laws have appeared in GMMflow-type constructions [RPL⁺26]; our contribution is to identify such feedback as the Eulerian Markov projection of a lifted labeled Schrödinger bridge and to separate *three distinct objects*: optimality in the augmented labeled space, feasibility after projection to the original state space, and the information gap between the lifted and unlabeled path-space laws. Numerical examples illustrate the lifted construction and projected Markov feedback for Gaussian-mixture steering.

Notation: We employ standard notation throughout the article. Let $\mathbb{N} := \{1, 2, \dots\}$ denote the set of positive integers. Given $d \in \mathbb{N}$, we denote the d -dimensional Euclidean space by \mathbb{R}^d , equipped with the standard inner product $(x, y) \mapsto x^\top y$ and norm $x \mapsto \|x\|$. For $p \in \mathbb{N}$, I_p denotes the $p \times p$ identity matrix. For $q \in \mathbb{N}$, \mathbb{S}^q , \mathbb{S}_+^q , and \mathbb{S}_{++}^q denote the sets of $q \times q$ real symmetric, real symmetric positive semidefinite, and real symmetric positive definite matrices, respectively. For $A \in \mathbb{S}_{++}^q$, $A^{1/2}$ denotes the unique positive definite square root of the matrix A . The trace and determinant of a square matrix A are denoted by $\text{tr}(A)$ and $\det(A)$, respectively. Given a metric space X , we write $\mathcal{B}(X)$ for its Borel sigma-algebra and $\mathcal{P}(X)$ for the set of probability measures on $(X, \mathcal{B}(X))$. If X and Y are metric spaces, $T : X \rightarrow Y$ is measurable, and $\mu \in \mathcal{P}(X)$, then the pushforward of μ by T , denoted by $T_\# \mu \in \mathcal{P}(Y)$, is defined by $\mathcal{B}(Y) \ni A \mapsto (T_\# \mu)(A) := \mu(T^{-1}(A))$. For $z \in X$, δ_z denotes the Dirac measure at z . For two probability measures μ, ν on a common measurable space X , we write $\mu \ll \nu$ to mean that μ is absolutely continuous with respect to ν . The support of a measure is denoted by $\text{supp}(\cdot)$. For a nonnegative matrix $\pi := (\pi_{ij})$ indexed by finite sets \mathcal{I} and \mathcal{J} , we write $\text{supp } \pi := \{(i, j) \in \mathcal{I} \times \mathcal{J} \mid \pi_{ij} > 0\}$. We use $\mathcal{N}(m, \Sigma)$ to denote the Gaussian law with mean m and covariance Σ , and also its density when the meaning is clear from context. The relative entropy of μ with respect to ν is denoted by $D_{\text{KL}}(\mu \parallel \nu) := \int_X \log \left(\frac{d\mu}{d\nu} \right) d\mu$ when $\mu \ll \nu$ and $+\infty$, otherwise. For a random variable X defined on a probability space with law \mathcal{Q} , we write $\text{Law}_{\mathcal{Q}}(X)$ for its distribution and $E^{\mathcal{Q}}[\cdot]$ for expectation under \mathcal{Q} . When the underlying law is clear from context, we write $E[\cdot]$.

§2. The stochastic optimal control problem

Fix $d \in \mathbb{N}$ and a noise level $\varepsilon > 0$. Let $\Omega := \mathcal{C}([0, 1]; \mathbb{R}^d)$ be the space of continuous paths equipped with the Borel σ -algebra, where Ω is endowed with the uniform topology. Let $\Omega \ni \omega \mapsto x_t(\omega) := \omega(t) \in \mathbb{R}^d$ be the canonical process on Ω .¹ We consider controlled diffusions on \mathbb{R}^d of the form

$$(1) \quad dx_t = u_t(x_t) dt + \sqrt{\varepsilon} dw_t \quad \text{for } t \in [0, 1],$$

with the following data:

$$((1)\text{-a}) \quad (w_t)_{t \in [0, 1]} \text{ is an } \mathbb{R}^d\text{-valued standard Brownian motion;}$$

¹All stochastic processes below may be realized on rich enough complete filtered probability spaces with suitably defined filtrations; however, since the analysis is carried out at the level of induced path laws, we work on the canonical path space Ω and identify each controlled diffusion with its law on Ω .

((1)-b) The drift u is taken from the regular feedback class \mathcal{U}_{reg} , consisting of Borel measurable maps

$$u : [0, 1] \times \mathbb{R}^d \longrightarrow \mathbb{R}^d, \quad [0, 1] \times \mathbb{R}^d \ni (\tau, \xi) \mapsto u_\tau(\xi) \in \mathbb{R}^d,$$

such that $u_t(\cdot)$ is locally Lipschitz in x , uniformly on compact sets with time-integrable local Lipschitz constants, and has at most linear growth in x . More precisely, for every $R > 0$, there exists $L_R \in L^1(0, 1)$ such that, for a.e. $t \in [0, 1]$,

$$\|u_t(x) - u_t(y)\| \leq L_R(t) \|x - y\| \quad \text{for all } \|x\|, \|y\| \leq R,$$

and there exists $a \in L^2(0, 1)$ such that, for all $x \in \mathbb{R}^d$ and for a.e. $t \in [0, 1]$,

$$\|u_t(x)\| \leq a(t)(1 + \|x\|).$$

Under the regularity assumptions ((1)-a)–((1)-b), for every initial law with finite second moment, (1) admits a *unique strong solution* [KS91, Chapter 5, Theorem 5.2.9], [YZ99, Chapter 1, §6.4], [Bor05]. In particular, the induced law of the process on Ω is well-defined.

Fix $N_1, N_2 \in \mathbb{N}$. Let $m_i^0, m_j^1 \in \mathbb{R}^d$ and $\Sigma_i^0, \Sigma_j^1 \in \mathbb{S}_{++}^d$. Consider the following weights that satisfy

$$\alpha_i^0, \alpha_j^1 > 0, \quad \sum_{i=1}^{N_1} \alpha_i^0 = 1, \quad \sum_{j=1}^{N_2} \alpha_j^1 = 1.$$

Let $\mathcal{I} := \{1, \dots, N_1\}$ and $\mathcal{J} := \{1, \dots, N_2\}$, and define the Gaussian densities

$$p_i^0 := \mathcal{N}(m_i^0, \Sigma_i^0), \quad p_j^1 := \mathcal{N}(m_j^1, \Sigma_j^1), \quad i \in \mathcal{I}, j \in \mathcal{J}.$$

The initial and terminal densities are $\xi \mapsto \rho_0(\xi)$ and $\xi \mapsto \rho_1(\xi)$, respectively, which are defined on \mathbb{R}^d , and have the Gaussian-mixture specification

$$(2) \quad \xi \mapsto \rho_0(\xi) := \sum_{i=1}^{N_1} \alpha_i^0 p_i^0(\xi), \quad \xi \mapsto \rho_1(\xi) := \sum_{j=1}^{N_2} \alpha_j^1 p_j^1(\xi).$$

We define the admissible control set associated with the endpoint pair (ρ_0, ρ_1) by

$$\mathcal{U}(\rho_0, \rho_1) := \left\{ u \in \mathcal{U}_{\text{reg}} \left| \begin{array}{l} \text{the solution of (1) with } x_0 \sim \rho_0 \text{ satisfies } x_1 \sim \rho_1, \\ \mathbb{E} \left[\int_0^1 \|u_t(x_t)\|^2 dt \right] < +\infty \end{array} \right. \right\}.$$

The stochastic density-control problem is

Problem 1

$$\inf_{u \in \mathcal{U}(\rho_0, \rho_1)} \mathbb{E} \left[\int_0^1 \frac{1}{2} \|u_t(x_t)\|^2 dt \right] = \inf_{u \in \mathcal{U}_{\text{reg}}} \mathbb{E} \left[\int_0^1 \frac{1}{2} \|u_t(x_t)\|^2 dt \right]$$

s. t. $\begin{cases} \text{dynamics (1), } x_0 \sim \rho_0, x_1 \sim \rho_1, \\ \mathbb{E} \int_0^1 \|u_t(x_t)\|^2 dt < +\infty. \end{cases}$

Remark 1 (Extension to linear stochastic control systems). *The lifted Schrödinger bridge construction which we will present in the sequel is not limited to the Brownian prior*

$$dx_t = u_t(x_t) dt + \sqrt{\varepsilon} dw_t,$$

and extends in the same spirit to linear stochastic systems of the form [CGP17, MAJTC25]

$$dx_t = A(t)x_t dt + B(t)v_t(x_t) dt + \sqrt{\varepsilon} B(t) dw_t,$$

with the usual problem data. In that case, the reference process is the uncontrolled linear diffusion, and the control cost in Problem 1 is measured in terms of the input v_t , not the total drift. The pairwise component bridges remain linear-Gaussian, so the Brownian pairwise formulas in the sequel are simply replaced by their corresponding linear-system

analogues. At the structural level, however, the rest of the theory in the sequel will remain unchanged: the lifted KL decomposition, the finite-dimensional entropic coupling problem, the Sinkhorn scaling form, the projected density construction, the energy bound, and the projection-gap identity all continue to hold in the same form.

§3. Main results

Problem 1 is posed on the original state space \mathbb{R}^d and is therefore unlabeled: the component indices $i \in \mathcal{I}$ and $j \in \mathcal{J}$ in the Gaussian-mixture representation are not observed state variables of the controlled diffusion. They only encode a chosen decomposition of the endpoint densities. In this section, we use these component labels as auxiliary variables to construct a lifted path-space formulation. This lifted formulation decomposes the mixture-to-mixture problem into pairwise component Schrödinger bridges coupled through a finite-dimensional transport plan.

We first recall the path-space relative-entropy representation of the stochastic control cost, then define the pairwise component bridges, and finally show that the lifted problem reduces exactly to a finite-dimensional entropic coupling problem over the mixture weights. This construction should be interpreted as an exact reduction of a labeled, lifted problem. Its relation to the original unlabeled density-control problem is addressed afterward through a projection identity.

§3.1. Uncontrolled reference law. Fix an initial law $\nu \in \mathcal{P}(\mathbb{R}^d)$ and let $\mathbb{R}^\nu \in \mathcal{P}(\Omega)$ denote the path law on Ω of the uncontrolled diffusion

$$(3) \quad dx_t = \sqrt{\varepsilon} dw_t \quad \text{with } \text{Law}(x_0) := \nu.$$

For probability measures \mathbb{Q} and \mathbb{R} on $(\Omega, \mathcal{B}(\Omega))$, recall the definition of KL divergence $D_{\text{KL}}(\mathbb{Q} \parallel \mathbb{R})$. Let $u \in \mathcal{U}_{\text{reg}}$ and let \mathbb{Q}^u denote the path law induced by the controlled diffusion

$$dx_t = u_t(x_t) dt + \sqrt{\varepsilon} dw_t \quad \text{with } \text{Law}(x_0) := \nu.$$

Whenever $\mathbb{Q}^u \ll \mathbb{R}^\nu$, Girsanov's theorem [CGP16] gives

$$(4) \quad D_{\text{KL}}(\mathbb{Q}^u \parallel \mathbb{R}^\nu) = \frac{1}{2\varepsilon} \mathbb{E}^{\mathbb{Q}^u} \left[\int_0^1 \|u_t(x_t)\|^2 dt \right].$$

Thus, the stochastic density-control cost in §2 can be represented as a path-space relative-entropy cost. In the sequel, this representation will be applied componentwise with $\nu = p_i^0$, yielding the pairwise Schrödinger bridges between the Gaussian components of the initial and terminal mixtures.

Remark 2 (Well-posedness of Problem 1). *Problem 1 is a stochastic optimal control problem with fixed initial and terminal marginals. Existence and duality results for such fixed-marginal stochastic control problems, including convex running costs, are classical; see, for example, [MT06, MT08, Mik21]. In the present Brownian setting, the Girsanov identity above identifies the quadratic cost with relative entropy with respect to the uncontrolled Brownian reference law, and the corresponding path-space formulation is the Brownian Schrödinger bridge problem; see also [CL94, L14, CGP16]. Since the endpoint densities considered here are finite mixtures of nondegenerate Gaussian densities, they are smooth, strictly positive, and have finite second moments.*

§3.2. Pairwise component SBs. In the mixture setting (2), each initial component p_i^0 gives rise to its own uncontrolled reference law. For each $i \in \mathcal{I}$, define $\mathbb{R}^i := \mathbb{R}^{p_i^0}$, i.e.,

R^i is the law of the uncontrolled diffusion (3) with $\nu = p_i^0$. For each $(i, j) \in \mathcal{F} \times \mathcal{F}$, define the pairwise component Schrödinger bridge by

$$(5) \quad P^{ij} \in \arg \min_{\{Q \in \mathcal{P}(\Omega) \mid \text{Law}_Q(x_0) = p_i^0, \text{Law}_Q(x_1) = p_j^1\}} \text{D}_{\text{KL}}(Q \| R^i).$$

Since p_i^0 and p_j^1 are nondegenerate Gaussian densities, this bridge is well defined. We denote by u^{ij} its optimal drift and by ρ_t^{ij} its time- t marginal density. Define the KL cost $\kappa_{ij} := \text{D}_{\text{KL}}(P^{ij} \| R^i)$, and the corresponding kinetic-energy cost by $C_{ij} := \varepsilon \kappa_{ij}$. We also have by the Girsanov identity

$$(6) \quad C_{ij} = \mathbb{E}^{P^{ij}} \left[\int_0^1 \frac{1}{2} \|u_t^{ij}(x_t)\|^2 dt \right],$$

i.e., C_{ij} is the minimum kinetic energy required to steer the initial Gaussian component p_i^0 to the terminal Gaussian component p_j^1 , relative to the uncontrolled Brownian reference initialized at p_i^0 .

§ 3.3. Closed-form pairwise Gaussian Schrödinger bridges. We now make the Gaussian structure of the pairwise component bridges explicit. Proposition 1 below is standard [BHCK23, CGP16] for Brownian Schrödinger bridges between nondegenerate Gaussian marginals, but we state the results here in the notation of our manuscript, since they will be used directly to compute the pairwise costs C_{ij} .

Fix $(i, j) \in \mathcal{F} \times \mathcal{F}$, and recall that

$$p_i^0 := \mathcal{N}(m_i^0, \Sigma_i^0), \quad p_j^1 := \mathcal{N}(m_j^1, \Sigma_j^1),$$

with $m_i^0, m_j^1 \in \mathbb{R}^d$ and $\Sigma_i^0, \Sigma_j^1 \in \mathbb{S}_{++}^d$. Let P^{ij} denote the pairwise Schrödinger bridge defined in (5), and let ρ_t^{ij} and u_t^{ij} denote its time- t marginal density and optimal drift, respectively. We first state the Gaussian endpoint coupling associated with P^{ij} .

Proposition 1 (Gaussian endpoint coupling for the pairwise bridge). *For each $(i, j) \in \mathcal{F} \times \mathcal{F}$, the pairwise bridge P^{ij} is Gaussian. In particular, the endpoint pair (x_0, x_1) under P^{ij} is jointly Gaussian:*

$$\text{Law}_{P^{ij}}(x_0, x_1) = \mathcal{N} \left(\begin{bmatrix} m_i^0 \\ m_j^1 \end{bmatrix}, \begin{bmatrix} \Sigma_i^0 & \Sigma_{01}^{ij} \\ (\Sigma_{01}^{ij})^\top & \Sigma_j^1 \end{bmatrix} \right),$$

where

$$\Sigma_{01}^{ij} := (\Sigma_i^0)^{1/2} \Xi_{ij} (\Sigma_i^0)^{-1/2} - \frac{\varepsilon}{2} I, \quad \Xi_{ij} := \left((\Sigma_i^0)^{1/2} \Sigma_j^1 (\Sigma_i^0)^{1/2} + \frac{\varepsilon^2}{4} I \right)^{1/2}.$$

Proposition 1 yields an explicit description of the (i, j) -bridge. The next result broadly adapts the technique given in [BHCK23, Theorem 3] to our setting to compute the component costs C_{ij} . A proof is included in Appendix 7.

Proposition 2 (Closed-form pairwise Gaussian bridge). *Fix $(i, j) \in \mathcal{F} \times \mathcal{F}$, and let Σ_{01}^{ij} be as in Proposition 1. Then $\Sigma_t^{ij} \in \mathbb{S}_{++}^d$ for every $t \in [0, 1]$ and the following hold.*

- (2-a) *For every $t \in [0, 1]$, the time- t marginal under P^{ij} is Gaussian $\rho_t^{ij} = \mathcal{N}(m_t^{ij}, \Sigma_t^{ij})$, with $m_t^{ij} := (1-t)m_i^0 + tm_j^1$ and $\Sigma_t^{ij} := (1-t)^2 \Sigma_i^0 + t^2 \Sigma_j^1 + t(1-t)(\Sigma_{01}^{ij} + (\Sigma_{01}^{ij})^\top + \varepsilon I)$.*

(2-b) For every $t \in [0, 1)$, the bridge drift admits the affine representation $x \mapsto u_t^{ij}(x) := A_t^{ij}(x - m_t^{ij}) + c_{ij}$ with $c_{ij} := m_j^1 - m_i^0$, where $A_t^{ij} := S_t^{ij}(\Sigma_t^{ij})^{-1}$ and $S_t^{ij} := (1-t)((\Sigma_{01}^{ij})^\top - \Sigma_i^0) + t(\Sigma_j^1 - \Sigma_{01}^{ij} - \varepsilon I)$.

(2-c) The pairwise kinetic-energy cost is

$$C_{ij} := \frac{1}{2} \int_{[0,1] \times \mathbb{R}^d} \rho_t^{ij}(x) \|u_t^{ij}(x)\|^2 dx dt = \frac{1}{2} \|m_j^1 - m_i^0\|^2 + \frac{1}{2} \int_0^1 \text{tr}(A_t^{ij} \Sigma_t^{ij} (A_t^{ij})^\top) dt.$$

§3.4. Lifting the mixture problem.

We first define a few objects needed in the sequel. A matrix $\pi := (\pi_{ij})_{i \in \mathcal{I}, j \in \mathcal{J}}$ is a *component coupling* for the mixture weights (α^0, α^1) if

$$(7) \quad \pi_{ij} \geq 0, \quad \sum_{j \in \mathcal{J}} \pi_{ij} = \alpha_i^0 \quad \text{for all } i \in \mathcal{I} \quad \text{and} \quad \sum_{i \in \mathcal{I}} \pi_{ij} = \alpha_j^1 \quad \text{for all } j \in \mathcal{J}.$$

We denote the set of all such couplings by $\Pi(\alpha^0, \alpha^1)$. Note that, π_{ij} is the fraction of total mass assigned to start from initial component i and end at terminal component j . The constraints (7) ensure that, aggregating over all terminal components, the total mass leaving component i equals α_i^0 , and aggregating over all initial components, the total mass arriving at component j equals α_j^1 .

Define a discrete label space $\mathcal{X} := \mathcal{I} \times \mathcal{J}$. Let Z be a \mathcal{X} -valued random variable with $\mathbb{P}(Z = (i, j)) = \pi_{ij}$. We lift the state space from trajectories Ω to the product space

$$\bar{\Omega} := \mathcal{X} \times \Omega = (\{1, \dots, N_1\} \times \{1, \dots, N_2\}) \times \mathcal{C}([0, 1]; \mathbb{R}^d),$$

and equip $\bar{\Omega}$ with $\mathcal{B}(\bar{\Omega})$. Observe that, a point in $\bar{\Omega}$ is a pair (z, ω) with $z = (i, j)$ and $[0, 1] \ni t \mapsto \omega(t) \in \mathbb{R}^d$ a continuous trajectory. We now define one of the chief objects: For $\pi \in \Pi(\alpha^0, \alpha^1)$, define a probability measure on $\bar{\Omega}$ by

$$(8) \quad \bar{\mathbb{P}}^\pi := \sum_{i \in \mathcal{I}} \sum_{j \in \mathcal{J}} \pi_{ij} \delta_{(i,j)} \otimes \mathbb{P}^{ij} \in \mathcal{P}(\bar{\Omega}).$$

In (8), $\delta_{(i,j)}$ denotes the Dirac measure on the discrete label space $\mathcal{X} := \mathcal{I} \times \mathcal{J}$ concentrated at the label (i, j) . Thus, $\delta_{(i,j)} \otimes \mathbb{P}^{ij}$ is the product probability measure on $(\mathcal{X} \times \Omega, \mathcal{B}(\mathcal{X}) \otimes \mathcal{B}(\Omega))$ satisfying

$$A \times B \mapsto (\delta_{(i,j)} \otimes \mathbb{P}^{ij})(A \times B) := \delta_{(i,j)}(A) \mathbb{P}^{ij}(B) \quad \text{for all } A \in \mathcal{B}(\mathcal{X}) \text{ and } B \in \mathcal{B}(\Omega),$$

where $\delta_{(i,j)}(A) = 1$ if $(i, j) \in A$, and $\delta_{(i,j)}(A) = 0$ otherwise. Consequently, if $x_{0:1} := \{t \mapsto x_t \mid t \in [0, 1]\}$, to sample $(Z, x_{0:1}) \sim \bar{\mathbb{P}}^\pi$ one needs to follow the two-step procedure: (i) draw $Z = (i, j)$ with probability π_{ij} ; (ii) conditional on $Z = (i, j)$, draw an entire trajectory $x_{0:1}$ from the pairwise bridge law \mathbb{P}^{ij} . Our first observation is that the endpoint constraints are satisfied by construction.

Proposition 3. *Let $\pi \in \Pi(\alpha^0, \alpha^1)$ and let $\rho_t^\pi(\cdot)$ denote the time- t marginal density of x_t under $\bar{\mathbb{P}}^\pi$. Then,*

$$(9) \quad x \mapsto \rho_t^\pi(x) := \sum_{i \in \mathcal{I}} \sum_{j \in \mathcal{J}} \pi_{ij} \rho_t^{ij}(x),$$

and, in particular, $\rho_0^\pi = \rho_0$ and $\rho_1^\pi = \rho_1$.

PROOF. By Definition (8), conditioning on $Z = (i, j)$ yields the pairwise law \mathbb{P}^{ij} . Therefore, the law of x_t under $\bar{\mathbb{P}}^\pi$ is the mixture of the laws under \mathbb{P}^{ij} with weights π_{ij} , giving (9). At $t = 0$, $\rho_0^{ij} = p_i^0$, hence

$$\rho_0^\pi = \sum_{(i,j) \in \mathcal{I} \times \mathcal{J}} \pi_{ij} p_i^0 = \sum_{i \in \mathcal{I}} \left(\sum_{j \in \mathcal{J}} \pi_{ij} \right) p_i^0 = \sum_{i \in \mathcal{I}} \alpha_i^0 p_i^0 = \rho_0.$$

Similarly, at $t = 1$, $\rho_1^{ij} = p_j^1$, hence,

$$\rho_1^\pi = \sum_{(i,j) \in \mathcal{I} \times \mathcal{J}} \pi_{ij} p_j^1 = \sum_{j \in \mathcal{J}} \left(\sum_{i \in \mathcal{I}} \pi_{ij} \right) p_j^1 = \sum_{j \in \mathcal{J}} \alpha_j^1 p_j^1 = \rho_1.$$

Thus, the lifted law $\bar{\mathbb{P}}^\pi$ satisfies the endpoints by construction. \square

We now endow the lifted construction with an entropic optimality criterion, which selects the component coupling π by comparing $\bar{\mathbb{P}}^\pi$ against a labeled reference law on $\bar{\Omega}$.

§ 3.4.1. *Augmented entropic formulation.* Let $\pi, \eta \in \Pi(\alpha^0, \alpha^1)$ with $\eta_{ij} > 0$. Define the standard KL divergence $D_{\text{KL}}(\pi \parallel \eta) := \sum_{i,j} \pi_{ij} \log\left(\frac{\pi_{ij}}{\eta_{ij}}\right)$. We now construct an augmented reference law in the lifted space $\bar{\Omega}$. Fix a strictly positive *prior coupling* $\eta \in \Pi(\alpha^0, \alpha^1)$ with $\eta_{ij} > 0$. Define the augmented (uncontrolled) measure

$$(10) \quad \bar{\mathbb{R}}^\eta := \sum_{i \in \mathcal{I}} \sum_{j \in \mathcal{J}} \eta_{ij} \delta_{(i,j)} \otimes \mathbb{R}^i \in \mathcal{P}(\bar{\Omega}).$$

The coupling η plays the role of a prior component assignment before accounting for the pairwise bridge costs. We now come to one of our main results.

Define the admissible lifted class

$$(11) \quad \mathcal{A}_{\text{lift}} := \left\{ \bar{\mathbb{Q}} := \sum_{i,j} \pi_{ij} \delta_{(i,j)} \otimes \mathbb{Q}^{ij} \in \mathcal{P}(\bar{\Omega}) \left| \begin{array}{l} \pi \in \Pi(\alpha^0, \alpha^1), \mathbb{Q}^{ij} \in \mathcal{P}(\Omega), \\ \text{Law}_{\mathbb{Q}^{ij}}(x_0) = p_i^0, \text{Law}_{\mathbb{Q}^{ij}}(x_1) = p_j^1. \end{array} \right. \right\}.$$

Theorem 1 (An exact lifted reduction). *Let $\eta \in \Pi(\alpha^0, \alpha^1)$ satisfy $\eta_{ij} > 0$ for all $(i, j) \in \mathcal{I} \times \mathcal{J}$, and define $\bar{\mathbb{R}}^\eta$ by (10). Consider the lifted problem*

$$(12) \quad \inf_{\bar{\mathbb{Q}} \in \mathcal{A}_{\text{lift}}} D_{\text{KL}}(\bar{\mathbb{Q}} \parallel \bar{\mathbb{R}}^\eta).$$

Then, we have the following finite-dimensional form

$$(13) \quad \inf_{\bar{\mathbb{Q}} \in \mathcal{A}_{\text{lift}}} D_{\text{KL}}(\bar{\mathbb{Q}} \parallel \bar{\mathbb{R}}^\eta) = \inf_{\pi \in \Pi(\alpha^0, \alpha^1)} \left\{ \sum_{i,j} \pi_{ij} \kappa_{ij} + D_{\text{KL}}(\pi \parallel \eta) \right\}.$$

Equivalently, in the kinetic-energy scaling representation

$$(14) \quad \inf_{\bar{\mathbb{Q}} \in \mathcal{A}_{\text{lift}}} \varepsilon D_{\text{KL}}(\bar{\mathbb{Q}} \parallel \bar{\mathbb{R}}^\eta) = \inf_{\pi \in \Pi(\alpha^0, \alpha^1)} \left\{ \sum_{i,j} \pi_{ij} C_{ij} + \varepsilon D_{\text{KL}}(\pi \parallel \eta) \right\}.$$

Moreover, for every fixed $\pi \in \Pi(\alpha^0, \alpha^1)$, the optimal conditional laws on every active pair (i, j) with $\pi_{ij} > 0$ are the pairwise bridges $\mathbb{Q}^{ij} = \mathbb{P}^{ij}$. Hence, for any optimal coupling π^ , an optimal lifted law is given by*

$$\bar{\mathbb{P}}^{\pi^*} = \sum_{i,j} \pi_{ij}^* \delta_{(i,j)} \otimes \mathbb{P}^{ij}.$$

If, in addition, $\pi_{ij}^ > 0$ for all (i, j) , then the optimal conditional laws are unique for all component pairs.*

PROOF. Let

$$\bar{\mathbb{Q}} = \sum_{i,j} \pi_{ij} \delta_{(i,j)} \otimes \mathbb{Q}^{ij} \in \mathcal{A}_{\text{lift}}$$

be arbitrary. We first prove the inequality “ \geq ” in (13). If $D_{\text{KL}}(\bar{\mathbb{Q}} \parallel \bar{\mathbb{R}}^\eta) = +\infty$, then the desired lower bound is immediate. Hence, assume that $D_{\text{KL}}(\bar{\mathbb{Q}} \parallel \bar{\mathbb{R}}^\eta) < +\infty$. In particular, $\bar{\mathbb{Q}} \ll \bar{\mathbb{R}}^\eta$. Since $\bar{\mathbb{R}}^\eta = \sum_{i,j} \eta_{ij} \delta_{(i,j)} \otimes \mathbb{R}^i$ and $\eta_{ij} > 0$ for every (i, j) , it follows that, for every active pair (i, j) with $\pi_{ij} > 0$, one has $\mathbb{Q}^{ij} \ll \mathbb{R}^i$. Indeed, if $B \in \mathcal{B}(\Omega)$

satisfies $R^i(B) = 0$, then $\bar{R}^\eta(\{(i, j)\} \times B) = \eta_{ij}R^i(B) = 0$. Since $\bar{Q} \ll \bar{R}^\eta$, this implies $0 = \bar{Q}(\{(i, j)\} \times B) = \pi_{ij}Q^{ij}(B)$. Thus, if $\pi_{ij} > 0$, then $Q^{ij}(B) = 0$, proving $Q^{ij} \ll R^i$.

Consequently, the standard chain rule for relative entropy [DE97, Theorem B.2.1] applies on the disjoint label-slice decomposition of $\bar{Q} = \mathcal{X} \times \Omega$, and gives

$$(15) \quad D_{\text{KL}}(\bar{Q} \parallel \bar{R}^\eta) = D_{\text{KL}}(\pi \parallel \eta) + \sum_{i,j} \pi_{ij} D_{\text{KL}}(Q^{ij} \parallel R^i).$$

For each pair (i, j) , admissibility gives $\text{Law}_{Q^{ij}}(x_0) = p_i^0$ and $\text{Law}_{Q^{ij}}(x_1) = p_j^1$. Hence, by the definition of the pairwise Schrödinger bridge P^{ij} , $D_{\text{KL}}(Q^{ij} \parallel R^i) \geq D_{\text{KL}}(P^{ij} \parallel R^i) = \kappa_{ij}$. Therefore, using (15), we have $D_{\text{KL}}(\bar{Q} \parallel \bar{R}^\eta) \geq D_{\text{KL}}(\pi \parallel \eta) + \sum_{i,j} \pi_{ij} \kappa_{ij}$. Since this holds for every $\bar{Q} \in \mathcal{A}_{\text{lift}}$, we obtain

$$(16) \quad \inf_{\bar{Q} \in \mathcal{A}_{\text{lift}}} D_{\text{KL}}(\bar{Q} \parallel \bar{R}^\eta) \geq \inf_{\pi \in \Pi(\alpha^0, \alpha^1)} \left\{ D_{\text{KL}}(\pi \parallel \eta) + \sum_{i,j} \pi_{ij} \kappa_{ij} \right\}.$$

We now prove the reverse inequality. Let $\pi \in \Pi(\alpha^0, \alpha^1)$ be arbitrary, and recall the definition of \bar{P}^π from (8). Since each P^{ij} satisfies $\text{Law}_{P^{ij}}(x_0) = p_i^0$ and $\text{Law}_{P^{ij}}(x_1) = p_j^1$, we have $\bar{P}^\pi \in \mathcal{A}_{\text{lift}}$. Applying the preceding KL decomposition (15) with $Q^{ij} = P^{ij}$ gives $D_{\text{KL}}(\bar{P}^\pi \parallel \bar{R}^\eta) = D_{\text{KL}}(\pi \parallel \eta) + \sum_{i,j} \pi_{ij} \kappa_{ij}$. Taking the infimum over $\pi \in \Pi(\alpha^0, \alpha^1)$, we obtain

$$(17) \quad \inf_{\bar{Q} \in \mathcal{A}_{\text{lift}}} D_{\text{KL}}(\bar{Q} \parallel \bar{R}^\eta) \leq \inf_{\pi \in \Pi(\alpha^0, \alpha^1)} \left\{ D_{\text{KL}}(\pi \parallel \eta) + \sum_{i,j} \pi_{ij} \kappa_{ij} \right\}.$$

Combining inequalities (16) and (17) yields

$$\inf_{\bar{Q} \in \mathcal{A}_{\text{lift}}} D_{\text{KL}}(\bar{Q} \parallel \bar{R}^\eta) = \inf_{\pi \in \Pi(\alpha^0, \alpha^1)} \left\{ D_{\text{KL}}(\pi \parallel \eta) + \sum_{i,j} \pi_{ij} \kappa_{ij} \right\}.$$

Multiplying both sides by ε , and using $C_{ij} = \varepsilon \kappa_{ij}$, yields (14).

Finally, fix $\pi \in \Pi(\alpha^0, \alpha^1)$. The term $D_{\text{KL}}(\pi \parallel \eta)$ is fixed, and the only part depending on the conditional path laws is $\sum_{i,j} \pi_{ij} D_{\text{KL}}(Q^{ij} \parallel R^i)$. For every active pair (i, j) with $\pi_{ij} > 0$, the conditional path law Q^{ij} must minimize the pairwise problem

$$\inf \{ D_{\text{KL}}(Q \parallel R^i) \mid Q \in \mathcal{P}(\Omega), \text{Law}_Q(x_0) = p_i^0, \text{Law}_Q(x_1) = p_j^1 \},$$

where Q is a generic path-space optimization variable²

This pairwise minimization problem has a unique solution. Indeed, its admissible set is convex, and $Q \mapsto D_{\text{KL}}(Q \parallel R^i)$ is strictly convex on the set of measures absolutely continuous with respect to R^i . Since the Gaussian bridge P^{ij} has finite entropy, every minimizer has finite entropy and hence is absolutely continuous with respect to R^i . Therefore, two distinct minimizers cannot exist. The unique minimizer is precisely the pairwise Schrödinger bridge P^{ij} . Hence, for any optimal coupling π^* , the optimal lifted law is

$$\bar{P}^{\pi^*} = \sum_{i,j} \pi_{ij}^* \delta_{(i,j)} \otimes P^{ij}.$$

If, in addition, $\pi_{ij}^* > 0$ for all (i, j) , then every conditional law is active, and therefore the optimal conditional laws are unique for all component pairs. The proof is complete. \square

Consequently, minimizing the lifted KL cost over $\pi \in \Pi(\alpha^0, \alpha^1)$ is equivalently written, in the kinetic-energy scaling of Theorem 1, as the finite-dimensional strictly

²By the definition of the pairwise component Schrödinger bridge in (5), the minimizer of this problem is precisely P^{ij} . Therefore, on every active pair, the optimal conditional law is $Q^{ij} = P^{ij}$.

convex program

(18)

$$\pi^* \in \arg \min_{\pi \in \Pi(\alpha^0, \alpha^1)} \left\{ \sum_{i,j} \pi_{ij} C_{ij} + \varepsilon D_{\text{KL}}(\pi \| \eta) \right\} = \arg \min_{\pi \in \Pi(\alpha^0, \alpha^1)} \left\{ \sum_{i,j} \pi_{ij} \kappa_{ij} + D_{\text{KL}}(\pi \| \eta) \right\}.$$

Theorem 1 reduces the lifted entropy minimization problem to a finite-dimensional entropic transport problem over $\Pi(\alpha^0, \alpha^1)$; we now record its optimality conditions and the corresponding Sinkhorn scaling form.

§ 3.4.2. *Optimality conditions and Sinkhorn form.* We can solve for π in (18) using Sinkhorn-type scaling. Recall that $\eta \in \Pi(\alpha^0, \alpha^1)$ is the fixed strictly positive prior coupling used to define the lifted reference law $\tilde{\mathbb{R}}^\eta$ in (10). Define the Gibbs kernel [PC20]

$$(19) \quad K_{ij} := \eta_{ij} \exp\left(-\frac{C_{ij}}{\varepsilon}\right).$$

Since $C_{ij} = \varepsilon \kappa_{ij}$, one has $K_{ij} = \eta_{ij} \exp(-\kappa_{ij})$. We have the following scaling form.

Proposition 4. *The unique optimizer π^* of (18) has the form*

$$(20) \quad \pi_{ij}^* = a_i K_{ij} b_j,$$

for some positive vectors $a \in \mathbb{R}^{N_1}$, $b \in \mathbb{R}^{N_2}$ chosen so that $\sum_j \pi_{ij}^* = \alpha_i^0$, and $\sum_i \pi_{ij}^* = \alpha_j^1$.

PROOF. Consider the Lagrangian for Problem (18)

$$\mathcal{L}(\pi, \lambda, \mu) = \sum_{i,j} \pi_{ij} C_{ij} + \varepsilon \sum_{i,j} \pi_{ij} \log\left(\frac{\pi_{ij}}{\eta_{ij}}\right) + \sum_i \lambda_i \left(\alpha_i^0 - \sum_j \pi_{ij}\right) + \sum_j \mu_j \left(\alpha_j^1 - \sum_i \pi_{ij}\right).$$

Since $\eta_{ij} > 0$ and the retained mixture weights are strictly positive, the minimizer is strictly positive. Hence, the first-order stationarity condition gives

$$0 = \frac{\partial \mathcal{L}}{\partial \pi_{ij}} = C_{ij} + \varepsilon \left(\log(\pi_{ij}/\eta_{ij}) + 1 \right) - \lambda_i - \mu_j.$$

Rearranging, we get $\log(\pi_{ij}/\eta_{ij}) = (\lambda_i + \mu_j - C_{ij})/\varepsilon - 1$. Exponentiating and absorbing constants into a_i and b_j , we obtain

$$\pi_{ij} = \eta_{ij} \exp\left(-\frac{C_{ij}}{\varepsilon}\right) \exp\left(\frac{\lambda_i}{\varepsilon} - \frac{1}{2}\right) \exp\left(\frac{\mu_j}{\varepsilon} - \frac{1}{2}\right) = a_i K_{ij} b_j.$$

This yields (20). The marginal constraints determine the scaling vectors a, b , up to the usual reciprocal scaling ambiguity $a \mapsto ca, b \mapsto c^{-1}b$. \square

Note that the scaling vectors (a, b) can be computed by alternating normalization:

$$a_i \leftarrow \frac{\alpha_i^0}{\sum_j K_{ij} b_j}, \quad b_j \leftarrow \frac{\alpha_j^1}{\sum_i K_{ij} a_i},$$

iterated to convergence. See [PC20, Chapter 3] for more details.

The preceding results solve the lifted labeled problem, but the original SB/density-control problem is posed on the unlabeled path space; we therefore next project the lifted law by discarding/forgetting the component label and quantify the resulting entropy discrepancy.

§3.5. Quantifying the gap. Theorem 1 is exact for the lifted problem. However, the original problem is unlabeled and is posed on the path space Ω , not on $\tilde{\Omega}$. To this end, let us define

$$\mathcal{P}_\Omega : \mathcal{X} \times \Omega \rightarrow \Omega \quad \text{with } \mathcal{X} \times \Omega \ni (z, \omega) \mapsto \mathcal{P}_\Omega(z, \omega) := \omega \in \Omega,$$

which is the map that projects label-trajectory pairs onto the original path space. Define the path-space marginal of the lifted law associated with π by

$$(21) \quad \mathbb{Q}^\pi := (\mathcal{P}_\Omega)_\# \bar{\mathbb{P}}^\pi \in \mathcal{P}(\Omega) \quad \text{where } (\mathcal{P}_\Omega)_\# : \mathcal{P}(\tilde{\Omega}) \rightarrow \mathcal{P}(\Omega).$$

Since $\bar{\mathbb{P}}^\pi = \sum_{i,j} \pi_{ij} \delta_{(i,j)} \otimes \mathbb{P}^{ij}$, we have $\mathbb{Q}^\pi = \sum_{i,j} \pi_{ij} \mathbb{P}^{ij}$. Indeed, for any $B \in \mathcal{B}(\Omega)$, the definition $\mathbb{Q}^\pi = (\mathcal{P}_\Omega)_\# \bar{\mathbb{P}}^\pi$ in (21) gives

$$\mathbb{Q}^\pi(B) = \bar{\mathbb{P}}^\pi(Z \times B) = \sum_{i,j} \pi_{ij} (\delta_{(i,j)} \otimes \mathbb{P}^{ij})(Z \times B) = \sum_{i,j} \pi_{ij} \mathbb{P}^{ij}(B).$$

Similarly, for any $B \in \mathcal{B}(\Omega)$, the path-space marginal of the augmented reference law is

$$(22) \quad (\mathcal{P}_\Omega)_\# \bar{\mathbb{R}}^\eta(B) = \bar{\mathbb{R}}^\eta(Z \times B) = \sum_{i,j} \eta_{ij} \mathbb{R}^i(B) = \sum_i \alpha_i^0 \mathbb{R}^i(B) =: \mathbb{R}^{\rho^0} \in \mathcal{P}(\Omega),$$

where we used $\sum_j \eta_{ij} = \alpha_i^0$.

Thus, projecting $\bar{\mathbb{R}}^\eta$ onto the original path space removes the auxiliary label and recovers the uncontrolled Brownian reference law initialized from the mixture ρ_0 . Similarly, the projected law $\mathbb{Q}^\pi := (\mathcal{P}_\Omega)_\# \bar{\mathbb{P}}^\pi$ has endpoint marginals ρ_0 and ρ_1 by Proposition 3. Hence, \mathbb{Q}^π is a feasible path-space law for the original unlabeled endpoint problem. However, feasibility after projection does not imply equality of the corresponding relative entropies. The lifted law retains the auxiliary label $Z = (i, j)$, whereas \mathbb{Q}^π is obtained after forgetting this label. Consequently, in general

$$D_{\text{KL}}(\bar{\mathbb{P}}^\pi \| \bar{\mathbb{R}}^\eta) \neq D_{\text{KL}}(\mathbb{Q}^\pi \| \mathbb{R}^{\rho^0}).$$

The discrepancy between these two quantities is precisely the conditional label-information term quantified below.

Theorem 2 (Projection-gap identity for the lifted bridge). *Let $\pi, \eta \in \Pi(\alpha^0, \alpha^1)$ and $\text{supp } \pi \subseteq \text{supp } \eta$. Recall the definitions $\bar{\mathbb{P}}^\pi := \sum_{i,j} \pi_{ij} \delta_{(i,j)} \otimes \mathbb{P}^{ij}$ and $\bar{\mathbb{R}}^\eta := \sum_{i,j} \eta_{ij} \delta_{(i,j)} \otimes \mathbb{R}^i$. Let $\mathbb{Q}^\pi := (\mathcal{P}_\Omega)_\# \bar{\mathbb{P}}^\pi$ and $\mathbb{R}^{\rho^0} := (\mathcal{P}_\Omega)_\# \bar{\mathbb{R}}^\eta$ be defined as in (21) and (22). Define the conditional label-information gap*

$$(23) \quad \mathcal{G}(\pi, \eta) := E^{\mathbb{Q}^\pi} \left[D_{\text{KL}}(\bar{\mathbb{P}}^\pi(Z | x_{0:1}) \| \bar{\mathbb{R}}^\eta(Z | x_{0:1})) \right].$$

Then, $\mathcal{G}(\pi, \eta) \geq 0$, and $D_{\text{KL}}(\bar{\mathbb{P}}^\pi \| \bar{\mathbb{R}}^\eta) = D_{\text{KL}}(\mathbb{Q}^\pi \| \mathbb{R}^{\rho^0}) + \mathcal{G}(\pi, \eta)$. Consequently,

$$(24) \quad D_{\text{KL}}(\mathbb{Q}^\pi \| \mathbb{R}^{\rho^0}) = \sum_{i,j} \pi_{ij} \kappa_{ij} + D_{\text{KL}}(\pi \| \eta) - \mathcal{G}(\pi, \eta),$$

which, since $C_{ij} = \varepsilon \kappa_{ij}$, is equivalent to

$$(25) \quad \varepsilon D_{\text{KL}}(\mathbb{Q}^\pi \| \mathbb{R}^{\rho^0}) = \sum_{i,j} \pi_{ij} C_{ij} + \varepsilon D_{\text{KL}}(\pi \| \eta) - \varepsilon \mathcal{G}(\pi, \eta).$$

PROOF. Since each pairwise bridge satisfies $\mathbb{P}^{ij} \ll \mathbb{R}^i$ on every active label pair and $\text{supp } \pi \subseteq \text{supp } \eta$, we have $\bar{\mathbb{P}}^\pi \ll \bar{\mathbb{R}}^\eta$. Applying the standard relative-entropy chain rule [DE97, Theorem B.2.1] under the projection $\mathcal{P}_\Omega : \mathcal{X} \times \Omega \rightarrow \Omega$ gives

$$D_{\text{KL}}(\bar{\mathbb{P}}^\pi \| \bar{\mathbb{R}}^\eta) = D_{\text{KL}}((\mathcal{P}_\Omega)_\# \bar{\mathbb{P}}^\pi \| (\mathcal{P}_\Omega)_\# \bar{\mathbb{R}}^\eta) + E^{\mathbb{Q}^\pi} \left[D_{\text{KL}}(\bar{\mathbb{P}}^\pi(Z | x_{0:1}) \| \bar{\mathbb{R}}^\eta(Z | x_{0:1})) \right].$$

By definition, $(\mathcal{P}_\Omega)_\# \bar{\mathbb{P}}^\pi = \mathbb{Q}^\pi$ and $(\mathcal{P}_\Omega)_\# \bar{\mathbb{R}}^\eta = \mathbb{R}^{\rho^0}$, and hence

$$D_{\text{KL}}(\bar{\mathbb{P}}^\pi \| \bar{\mathbb{R}}^\eta) = D_{\text{KL}}(\mathbb{Q}^\pi \| \mathbb{R}^{\rho^0}) + \mathcal{G}(\pi, \eta).$$

The nonnegativity of $\mathcal{G}(\pi, \eta)$ follows from the nonnegativity of the relative entropy.

Finally, applying the label-sliced KL decomposition from (15) in Theorem 1, with $\mathbf{Q}^{ij} = \mathbf{P}^{ij}$, we obtain $D_{\text{KL}}(\bar{\mathbf{P}}^\pi \|\bar{\mathbf{R}}^\eta) = D_{\text{KL}}(\pi \|\eta) + \sum_{i,j} \pi_{ij} \kappa_{ij}$. Substituting this into the projection identity gives

$$(26) \quad D_{\text{KL}}(\mathbf{Q}^\pi \|\mathbf{R}^{\rho_0}) = \sum_{i,j} \pi_{ij} \kappa_{ij} + D_{\text{KL}}(\pi \|\eta) - \mathcal{G}(\pi, \eta).$$

Multiplying by ε , and using $C_{ij} = \varepsilon \kappa_{ij}$, gives the kinetic-energy-scaled identity. \square

Thus, the lifted objective equals the unlabeled path-space objective only up to the nonnegative gap term $\mathcal{G}(\pi, \eta)$. In general, this term does not vanish, and therefore, one cannot identify the lifted labeled problem with the original unlabeled problem without additional structure.

Remark 3. *Since $\mathcal{G}(\pi, \eta)$ is an expected conditional relative entropy, it is nonnegative. Moreover, $\mathcal{G}(\pi, \eta) = 0$ if and only if the two posterior distributions of the label $Z = (i, j)$, conditioned on the full path $x_{0:1}$ (recall that $x_{0:1} := \{t \mapsto x_t \mid t \in [0, 1]\}$), coincide \mathbf{Q}^π -almost surely. More precisely, $\mathcal{G}(\pi, \eta) = 0$ if and only if, for \mathbf{Q}^π -a.e. path $\omega \in \Omega$,*

$$\bar{\mathbf{P}}^\pi(Z = (i, j) \mid x_{0:1} = \omega) = \bar{\mathbf{R}}^\eta(Z = (i, j) \mid x_{0:1} = \omega)$$

for every $(i, j) \in \mathcal{F} \times \mathcal{F}$. This translates, after choosing Radon–Nikodym versions of the posterior densities, to

$$\frac{d(\pi_{ij} \mathbf{P}^{ij})}{d\mathbf{Q}^\pi}(\omega) = \frac{d(\eta_{ij} \mathbf{R}^i)}{d\mathbf{R}^{\rho_0}}(\omega) \quad \text{for all } (i, j) \text{ and for } \mathbf{Q}^\pi\text{-a.e. } \omega.$$

Under $\bar{\mathbf{P}}^\pi$, the label (i, j) determines both the initial component and the terminal component of the pairwise bridge. Under $\bar{\mathbf{R}}^\eta$, the path is generated by the uncontrolled law \mathbf{R}^i , which depends on i but not dynamically on j . Therefore, the posterior label distribution inferred from a full controlled bridge path need not agree with the posterior label distribution inferred from an uncontrolled reference path. Thus, except for specially aligned cases (see Proposition 5), one expects $\mathcal{G}(\pi, \eta) > 0$. Consequently, one should be careful while identifying the lifted labeled objective with the original unlabeled path-space objective.

Proposition 5 (A common path-potential condition for zero projection gap). *Let $\pi, \eta \in \Pi(\alpha^0, \alpha^1)$, and suppose that they have the same support $\mathcal{A} := \text{supp } \pi = \text{supp } \eta = \{(i, j) \in \mathcal{F} \times \mathcal{F} \mid \pi_{ij} > 0\} = \{(i, j) \in \mathcal{F} \times \mathcal{F} \mid \eta_{ij} > 0\}$. Assume that, for every $(i, j) \in \mathcal{A}$, one has $\mathbf{P}^{ij} \ll \mathbf{R}^i$ and that there exist a nonnegative measurable function $h : \Omega \rightarrow [0, +\infty)$ and constants $c_{ij} > 0$, $(i, j) \in \mathcal{A}$, such that*

$$(27) \quad \frac{d\mathbf{P}^{ij}}{d\mathbf{R}^i}(\omega) = c_{ij} h(\omega) \quad \text{for } \mathbf{R}^i\text{-a.e. } \omega \text{ with } (i, j) \in \mathcal{A}.$$

Assume, moreover, that the constants are compatible with the lifted prior in the sense that there exists $\lambda > 0$ such that $\pi_{ij} c_{ij} = \lambda \eta_{ij}$ for $(i, j) \in \mathcal{A}$. Then, the projection gap vanishes, i.e., $\mathcal{G}(\pi, \eta) = 0$.

PROOF. Recall Definitions (8) and (10). Since $\text{supp } \pi = \text{supp } \eta = \mathcal{A}$ and $\mathbf{P}^{ij} \ll \mathbf{R}^i$ for every $(i, j) \in \mathcal{A}$, we have $\bar{\mathbf{P}}^\pi \ll \bar{\mathbf{R}}^\eta$. Also recall the projections (21) and (22). From the projection-gap identity, we have that

$$\mathcal{G}(\pi, \eta) = \mathbf{E}^{\mathbf{Q}^\pi} \left[D_{\text{KL}}(\bar{\mathbf{P}}^\pi(Z \mid x_{0:1}) \|\bar{\mathbf{R}}^\eta(Z \mid x_{0:1})) \right].$$

It is therefore enough to show that the two posterior label distributions coincide \mathbf{Q}^π -a.e. Let $M := \sum_{(i,j) \in \mathcal{A}} \eta_{ij} \mathbf{R}^i$. For each i , write $r_i := \frac{d\mathbf{R}^i}{dM}$. Using $\frac{d\mathbf{P}^{ij}}{d\mathbf{R}^i} = c_{ij} h$, the posterior label

distribution under the lifted controlled law is, for \mathbb{Q}^π -a.e. ω ,

$$\bar{\mathbb{P}}^\pi(Z = (i, j) \mid \omega) = \frac{\pi_{ij} c_{ij} h(\omega) r_i(\omega)}{\sum_{(k, \ell) \in \mathcal{A}} \pi_{k\ell} c_{k\ell} h(\omega) r_k(\omega)}.$$

Similarly, the posterior label distribution under the lifted reference law is

$$\bar{\mathbb{R}}^\eta(Z = (i, j) \mid \omega) = \frac{\eta_{ij} r_i(\omega)}{\sum_{(k, \ell) \in \mathcal{A}} \eta_{k\ell} r_k(\omega)}.$$

By the compatibility condition $\pi_{ij} c_{ij} = \lambda \eta_{ij}$ for $(i, j) \in \mathcal{A}$, the numerator and denominator in the first expression are both multiplied by the same factor $\lambda h(\omega)$. Hence,

$$\bar{\mathbb{P}}^\pi(Z = (i, j) \mid x_{0:1} = \omega) = \bar{\mathbb{R}}^\eta(Z = (i, j) \mid x_{0:1} = \omega),$$

for every $(i, j) \in \mathcal{A}$, \mathbb{Q}^π -a.e. ω . Therefore, the conditional relative entropy inside the definition of $\mathcal{G}(\pi, \eta)$ is zero \mathbb{Q}^π -a.e., and hence $\mathcal{G}(\pi, \eta) = 0$. \square

Remark 4 (Interpretation and a non-vacuous zero-gap class). *Proposition 5 is a path-space statement. Assumption (27) is on the likelihood ratios of the pairwise Schrödinger bridge laws. The reason the projection gap vanishes in that case is that, after observing the projected path $\omega = x_{0:1}$, the same factor $h(\omega)$ appears in all active posterior label weights and cancels during normalization. The compatibility condition $\pi_{ij} c_{ij} = \lambda \eta_{ij}$ for $(i, j) \in \mathcal{A}$, then makes the posterior label distribution under the lifted controlled law coincide with the posterior label distribution under the lifted reference law. Hence, the conditional label-information term is zero.*

The condition (27), together with the compatibility condition $\pi_{ij} c_{ij} = \lambda \eta_{ij}$ for $(i, j) \in \mathcal{A}$, is not vacuous. A simple Gaussian-mixture class satisfying this condition is obtained from a common translation drift. For example, let $\varepsilon > 0$ and $N_1 = N_2 = N$, let the active assignment graph be diagonal, $\mathcal{A} = \{(i, i) \mid i = 1, \dots, N\}$, and take $\pi_{ii} = \eta_{ii} = \alpha_i^0$ for all $i = 1, \dots, N$. Fix $v \in \mathbb{R}^d$, and let $p_i^0 = \mathcal{N}(m_i^0, \Sigma_i^0)$, and $p_i^1 = \mathcal{N}(m_i^0 + v, \Sigma_i^0 + \varepsilon I)$. Consider the controlled Brownian dynamics

$$dx_t = v dt + \sqrt{\varepsilon} dw_t \quad \text{with } x_0 \sim p_i^0.$$

Its path law will be denoted by \mathbb{P}^{ii} . Since the drift is constant, Girsanov's formula gives, with respect to the uncontrolled reference law \mathbb{R}^i ,

$$\frac{d\mathbb{P}^{ii}}{d\mathbb{R}^i}(\omega) = \exp\left(\frac{1}{\varepsilon} v^\top (x_1(\omega) - x_0(\omega)) - \frac{1}{2\varepsilon} \|v\|^2\right).$$

Therefore, Proposition 5 applies with

$$(28) \quad \omega \mapsto h(\omega) := \exp\left(\frac{1}{\varepsilon} v^\top (x_1(\omega) - x_0(\omega)) - \frac{1}{2\varepsilon} \|v\|^2\right) \quad \text{with } c_{ii} = 1.$$

Since $\pi_{ii} = \eta_{ii}$, the compatibility condition holds with $\lambda = 1$. Note that \mathbb{P}^{ii} is indeed the pairwise Schrödinger bridge from p_i^0 to p_i^1 . Under the above controlled dynamics, $x_1 \sim \mathcal{N}(m_i^0 + v, \Sigma_i^0 + \varepsilon I) = p_i^1$. Moreover, for any admissible drift u steering p_i^0 to p_i^1 , the mean displacement satisfies $\mathbb{E}\left[\int_0^1 u_t(x_t) dt\right] = v$. Hence, Jensen's inequality gives

$$\mathbb{E}\left[\int_0^1 \frac{1}{2} \|u_t(x_t)\|^2 dt\right] \geq \frac{1}{2} \left\| \mathbb{E}\left[\int_0^1 u_t(x_t) dt\right] \right\|^2 = \frac{1}{2} \|v\|^2.$$

The constant drift $u_t \equiv v$ attains this lower bound. Therefore, it is optimal, and the corresponding path law is the pairwise Schrödinger bridge \mathbb{P}^{ii} . Consequently, for this prescribed-assignment Gaussian-mixture transformation, $\mathcal{G}(\pi, \eta) = 0$. This example does not collapse the mixture to a single Gaussian: the source means m_i^0 , and covariances Σ_i^0 may still vary with i . In this example, Assumption (27) simply says that all active

subpopulations undergo the same Brownian translation mechanism, so their pairwise bridge likelihood ratios share the common path-dependent factor h given in (28).

Remark 5 (A canonical choice of the prior coupling). *The choice of the prior coupling η should respect the prescribed marginals α^0 and α^1 . In particular, the entrywise uniform matrix $\eta_{ij} = 1/N_1N_2$ belongs to $\Pi(\alpha^0, \alpha^1)$ only in the special case where both mixture weights are uniform, i.e., $\alpha_i^0 = 1/N_1$, and $\alpha_j^1 = 1/N_2$. For general mixture weights, a natural neutral choice is, instead, the product coupling*

$$\eta_{ij} := \alpha_i^0 \alpha_j^1.$$

This corresponds to an independent prior between the source label $I \in \mathcal{I}$ and the target label $J \in \mathcal{J}$. This choice has a useful information-theoretic interpretation. Since $\pi \in \Pi(\alpha^0, \alpha^1)$, its marginals are fixed and equal to α^0 and α^1 . Therefore,

$$D_{\text{KL}}(\pi \| \alpha^0 \otimes \alpha^1) = \sum_{i,j} \pi_{ij} \log \left(\frac{\pi_{ij}}{\alpha_i^0 \alpha_j^1} \right) =: \text{MI}_\pi(I; J),$$

where $\text{MI}_\pi(I; J)$ denotes the mutual information between the initial component label I and the terminal component label J under the joint law π . Hence, for the independent prior $\eta = \alpha^0 \otimes \alpha^1$, the finite-dimensional problem becomes

$$\min_{\pi \in \Pi(\alpha^0, \alpha^1)} \left\{ \sum_{i,j} \pi_{ij} C_{ij} + \varepsilon \text{MI}_\pi(I; J) \right\}.$$

Thus, the first term favors low-energy component-to-component bridges, while the second term penalizes excessive dependence between source and target labels. The optimizer creates a structured assignment only when the reduction in pairwise bridge cost justifies the associated information cost. In this sense, $\eta = \alpha^0 \otimes \alpha^1$ is a canonical default choice when no prior component-assignment information is available. Moreover, the lifted formulation is not restricted to this neutral product prior — it is a natural benefit of our approach. This feature is illustrated numerically in §4.2.3, Figure 7.

The identity (26) above quantifies the loss incurred when the label coordinate is removed from the lifted law. It compares the labeled law $\bar{\mathbb{P}}^\pi$ on $\mathcal{X} \times \Omega$ with the unlabeled path law \mathbb{Q}^π on Ω . However, \mathbb{Q}^π is still a path-space object and, in general, retains *hidden memory* of the source–target label through the observed trajectory. Thus, \mathbb{Q}^π should not automatically be identified with the law of a Markov diffusion driven by a state-feedback drift. Following [RPL⁺26], we next construct such a state-feedback drift at the Eulerian level and later quantify the additional passage from the generally non-Markov path law \mathbb{Q}^π to the Markov law generated by this feedback.

§ 3.6. Projecting back: regularity and feasibility. We now show that the standard posterior-averaged mixture feedback [RPL⁺26] arises canonically from the lifted labeled law. Thus, the following construction should not be viewed as an independent ansatz; it is the Eulerian Markov projection of $\bar{\mathbb{P}}^\pi$. Fix $\pi \in \Pi(\alpha^0, \alpha^1)$, and consider the lifted law $\bar{\mathbb{P}}^\pi$. For every Borel set $A \in \mathcal{B}(\mathbb{R}^d)$, the joint law of the label Z and the state x_t satisfies

$$\bar{\mathbb{P}}^\pi(Z = (i, j), x_t \in A) = \pi_{ij} \int_A \rho_t^{ij}(x) dx.$$

Consequently, after forgetting the label, the time- t state density is

$$(29) \quad x \mapsto \rho_t^\pi(x) := \sum_{i,j} \pi_{ij} \rho_t^{ij}(x).$$

Moreover, the conditional probability of the hidden label given the current state is

$$(30) \quad \gamma_{ij}(t, x) := \bar{\mathbb{P}}^\pi(Z = (i, j) \mid x_t = x) = \frac{\pi_{ij} \rho_t^{ij}(x)}{\rho_t^\pi(x)}.$$

Since the drift under the conditional bridge \mathbb{P}^{ij} is u_t^{ij} , the state-only Markov drift induced by the lifted construction is obtained by posterior averaging over the unobserved label

$$(31) \quad x \mapsto \bar{u}_t^\pi(x) := \sum_{i,j} \gamma_{ij}(t, x) u_t^{ij}(x) = \frac{\sum_{i,j} \pi_{ij} \rho_t^{ij}(x) u_t^{ij}(x)}{\rho_t^\pi(x)}.$$

Equivalently, we have

$$\rho_t^\pi(x) \bar{u}_t^\pi(x) = \sum_{i,j} \pi_{ij} \rho_t^{ij}(x) u_t^{ij}(x).$$

This identity is the key reason why the pair $(\rho_t^\pi, \bar{u}_t^\pi)$ satisfies the Fokker–Planck equation after summing the componentwise equations, which we will show later in Proposition 6. We also note that the objects in (29)–(31) are algebraically identical to those employed in the Gaussian-mixture bridge constructions in [RPL⁺26]. The contribution here is not the formulas themselves, but their derivation from the lifted path-space law and its role in the projection analysis developed above.

Lemma 1 (Regularity of the projected drift). *Let $\pi \in \Pi(\alpha^0, \alpha^1)$, and recall the expressions (29), (30), and (31). Then, $\bar{u}^\pi \in \mathcal{U}_{\text{reg}}$. Specifically, for every $R > 0$, there exists $L_R(\cdot) \in L^1(0, 1)$ such that*

$$\|\bar{u}_t^\pi(x) - \bar{u}_t^\pi(y)\| \leq L_R(t) \|x - y\| \quad \text{with } \|x\|, \|y\| \leq R,$$

for a.e. $t \in [0, 1]$, and $a_\pi(\cdot) \in L^2(0, 1)$ such that

$$\|\bar{u}_t^\pi(x)\| \leq a_\pi(t)(1 + \|x\|) \quad \text{for } x \in \mathbb{R}^d,$$

for a.e. $t \in [0, 1]$.

PROOF. Recall from Proposition 2 that, for each $(i, j) \in \mathcal{I} \times \mathcal{J}$, the density $x \mapsto \rho_t^{ij}(x)$ is smooth and strictly positive, while the drift has the affine form

$$x \mapsto u_t^{ij}(x) = A_t^{ij}(x - m_t^{ij}) + c^{ij} \quad \text{for } t \in [0, 1].$$

Moreover, by the explicit formulas for the pairwise Gaussian bridge in Section 3.3, the maps $t \mapsto m_t^{ij}$, $t \mapsto S_t^{ij}$, and $t \mapsto \Sigma_t^{ij}$ are continuous on $[0, 1]$, with $\Sigma_t^{ij} \in \mathbb{S}_{++}^d$ for every $t \in [0, 1]$. Hence, $t \mapsto (\Sigma_t^{ij})^{-1}$ is continuous and uniformly bounded on $[0, 1]$. Since $A_t^{ij} = S_t^{ij}(\Sigma_t^{ij})^{-1}$, it follows that $t \mapsto A_t^{ij}$ is uniformly bounded on $[0, 1]$.

We first prove the linear-growth estimate. For each (i, j) , the affine representation gives

$$\|u_t^{ij}(x)\| \leq \|A_t^{ij}\| \|x\| + \|A_t^{ij} m_t^{ij}\| + \|c^{ij}\|.$$

Thus, setting $a_{ij}(t) := \|A_t^{ij}\| + \|A_t^{ij} m_t^{ij}\| + \|c^{ij}\|$, we have

$$\|u_t^{ij}(x)\| \leq a_{ij}(t)(1 + \|x\|).$$

By the boundedness of A_t^{ij} , m_t^{ij} , and c^{ij} , each a_{ij} belongs to $L^\infty(0, 1)$, hence also to $L^2(0, 1)$. Since there are only finitely many component pairs, $a_\pi(t) := \max_{i,j} a_{ij}(t)$ is bounded and thus belongs to $L^2(0, 1)$. Using the facts that $\gamma_{ij}^\pi(t, x) \geq 0$ and $\sum_{i,j} \gamma_{ij}^\pi(t, x) = 1$, we obtain

$$\|\bar{u}_t^\pi(x)\| \leq \sum_{i,j} \gamma_{ij}^\pi(t, x) \|u_t^{ij}(x)\| \leq a_\pi(t)(1 + \|x\|).$$

This proves the linear-growth condition.

It remains to prove the local Lipschitz condition. For a fixed $R > 0$, we denote by $\mathbf{B}_R := \{x \in \mathbb{R}^d \mid \|x\| \leq R\}$, the closed Euclidean ball of radius R centered at the origin. Observe that:

- Since each ρ_t^{ij} is a smooth positive Gaussian density and $\rho_t^\pi = \sum_{i,j} \pi_{ij} \rho_t^{ij}$, the function $(t, x) \mapsto \rho_t^\pi(x)$ is continuous and strictly positive on the compact set $[0, 1] \times \mathbf{B}_R$. Therefore, ρ_t^π has a positive minimum on this compact set [San23, Chapter 1]. Consequently, each posterior weight $x \mapsto \gamma_{ij}^\pi(t, x)$ is continuously differentiable in x , and $\nabla_x \gamma_{ij}^\pi$ is uniformly bounded on $[0, 1] \times \mathbf{B}_R$.
- Since u_t^{ij} is affine with uniformly bounded affine coefficients, both u_t^{ij} and $\nabla_x u_t^{ij} = A_t^{ij}$ are uniformly bounded on $[0, 1] \times \mathbf{B}_R$. Differentiating \bar{u}_t^π with respect to x , we get

$$\nabla_x \bar{u}_t^\pi(x) = \sum_{i,j} \left[u_t^{ij}(x) \otimes \nabla_x \gamma_{ij}^\pi(t, x) + \gamma_{ij}^\pi(t, x) A_t^{ij} \right].$$

The right-hand side is uniformly bounded on $[0, 1] \times \mathbf{B}_R$. Hence, there exists a constant $C_R < +\infty$ such that

$$\sup_{t \in [0, 1]} \sup_{x \in \mathbf{B}_R} \|\nabla_x \bar{u}_t^\pi(x)\| \leq C_R.$$

From the mean-value theorem [Rud76, Chapter 5]

$$\|\bar{u}_t^\pi(x) - \bar{u}_t^\pi(y)\| \leq C_R \|x - y\| \quad \text{with } x, y \in \mathbf{B}_R.$$

Thus, we may choose $t \mapsto L_R(t) := C_R$. Therefore, \bar{u}^π satisfies the local Lipschitz condition required in \mathcal{U}_{reg} . Combining the preceding linear-growth estimate and the local-Lipschitz estimate, we conclude that $\bar{u}^\pi \in \mathcal{U}_{\text{reg}}$. The proof is complete. \square

§ 3.6.1. *Feasibility of the projected drift.* Having constructed the posterior-averaged drift \bar{u}^π , we state the corresponding feasibility and energy properties. These are direct consequences of the componentwise Fokker–Planck equations and the convexity of the kinetic energy, and are included to make the connection with Problem 1 explicit.

Proposition 6 (Projected feasibility and energy bound). *Let $\pi \in \Pi(\alpha^0, \alpha^1)$, and suppose that the posterior-averaged drift \bar{u}^π belongs to \mathcal{U}_{reg} . Then, the pair $(\rho_t^\pi, \bar{u}_t^\pi)$ satisfies*

$$\partial_t \rho_t^\pi + \nabla \cdot (\rho_t^\pi \bar{u}_t^\pi) - \frac{\varepsilon}{2} \Delta \rho_t^\pi = 0,$$

on $(0, 1) \times \mathbb{R}^d$. Moreover, $\rho_0^\pi = \rho_0$, $\rho_1^\pi = \rho_1$. Furthermore, the projected Markov feedback satisfies the kinetic-energy bound

$$\mathcal{F}_{\text{proj}}(\pi) := \int_0^1 \int_{\mathbb{R}^d} \frac{1}{2} \rho_t^\pi(x) \|\bar{u}_t^\pi(x)\|^2 dx dt \leq \mathcal{F}_{\text{lift}}(\pi) := \sum_{i,j} \pi_{ij} C_{ij}.$$

PROOF. By definition, for each (i, j) , the pairwise bridge density ρ_t^{ij} and corresponding drift u_t^{ij} satisfy

$$\partial_t \rho_t^{ij} + \nabla \cdot (\rho_t^{ij} u_t^{ij}) - \frac{\varepsilon}{2} \Delta \rho_t^{ij} = 0.$$

Multiplying by π_{ij} and summing over (i, j) , we obtain

$$\partial_t \left(\sum_{i,j} \pi_{ij} \rho_t^{ij} \right) + \nabla \cdot \left(\sum_{i,j} \pi_{ij} \rho_t^{ij} u_t^{ij} \right) - \frac{\varepsilon}{2} \Delta \left(\sum_{i,j} \pi_{ij} \rho_t^{ij} \right) = 0.$$

By definition, $\rho_t^\pi = \sum_{i,j} \pi_{ij} \rho_t^{ij}$. Moreover, from (31), $\rho_t^\pi \bar{u}_t^\pi = \sum_{i,j} \pi_{ij} \rho_t^{ij} u_t^{ij}$. Substituting these identities yields $\partial_t \rho_t^\pi + \nabla \cdot (\rho_t^\pi \bar{u}_t^\pi) - \frac{\varepsilon}{2} \Delta \rho_t^\pi = 0$. The endpoint identities follow from

Proposition 3. It remains to prove the energy bound. Applying Jensen's inequality on $\bar{u}_t^\pi(x)$ gives

$$\|\bar{u}_t^\pi(x)\|^2 \leq \sum_{i,j} \gamma_{ij}^\pi(t,x) \|u_t^{ij}(x)\|^2.$$

Multiplying by $\rho_t^\pi(x)$ and using $\rho_t^\pi(x) \gamma_{ij}^\pi(t,x) = \pi_{ij} \rho_t^{ij}(x)$, we obtain

$$\rho_t^\pi(x) \|\bar{u}_t^\pi(x)\|^2 \leq \sum_{i,j} \pi_{ij} \rho_t^{ij}(x) \|u_t^{ij}(x)\|^2.$$

Finally, integrating over $[0, 1] \times \mathbb{R}^d$ gives $\mathcal{F}_{\text{proj}}(\pi) \leq \mathcal{F}_{\text{lift}}(\pi)$. \square

We have the following immediate corollary.

Corollary 1 (Admissibility for Problem 1). *For every $\pi \in \Pi(\alpha^0, \alpha^1)$, the posterior-averaged drift \bar{u}^π belongs to $\mathcal{U}(\rho_0, \rho_1)$. In particular, the admissible set in Problem 1 is nonempty.*

PROOF. By Lemma 1, $\bar{u}^\pi \in \mathcal{U}_{\text{reg}}$, so the SDE $dx_t = \bar{u}_t^\pi(x_t) dt + \sqrt{\varepsilon} dw_t$, with $x_0 \sim \rho_0$ admits a unique strong solution. Its one-time marginals solve the Fokker–Planck equation associated with \bar{u}^π . By Proposition 6, the explicitly constructed density ρ_t^π solves the same Fokker–Planck equation and satisfies $\rho_0^\pi = \rho_0$. By uniqueness of the marginal/Fokker–Planck flow for drifts in \mathcal{U}_{reg} , the law of x_t has density ρ_t^π . In particular, $x_1 \sim \rho_1$. Finally, Proposition 6 gives

$$\mathbb{E} \left[\int_0^1 \|\bar{u}_t^\pi(x_t)\|^2 dt \right] = \int_0^1 \int_{\mathbb{R}^d} \rho_t^\pi(x) \|\bar{u}_t^\pi(x)\|^2 dx dt < +\infty.$$

Hence, $\bar{u}^\pi \in \mathcal{U}(\rho_0, \rho_1)$. \square

Consequently, Problem 1 is feasible, and the projected construction gives an explicit finite-energy admissible feedback.

§ 3.7. Mean-Field Extension. The lifted construction also provides a natural way to formulate the mean-field Schrödinger bridge problem [RPT25, ECH26] with Gaussian-mixture endpoints. To this end, consider the linear McKean–Vlasov dynamics

$$dx_t = A_t x_t dt + \bar{A}_t \bar{x}_t dt + B_t u_t(x_t) dt + D_t dw_t, \quad \text{with } \bar{x}_t := \mathbb{E}[x_t],$$

with the same prescribed Gaussian-mixture boundary distributions ρ_0 and ρ_1 . Let

$$\hat{x}_0 := \sum_{i \in \mathcal{I}} \alpha_i^0 m_i^0, \quad \hat{x}_1 := \sum_{j \in \mathcal{J}} \alpha_j^1 m_j^1,$$

denote the endpoint means. In the unconstrained case, the mean-field term can be separated by writing $x_t = \bar{x}_t + \tilde{x}_t$, and $u_t = \bar{u}_t + \tilde{u}_t$, where $\bar{x}_t := \mathbb{E}[x_t]$, $\bar{u}_t := \mathbb{E}[u_t(x_t)]$, and $\mathbb{E}[\tilde{x}_t] = \mathbb{E}[\tilde{u}_t] = 0$. This yields the deterministic mean-steering problem

$$\dot{\bar{x}}_t = (A_t + \bar{A}_t) \bar{x}_t + B_t \bar{u}_t \quad \bar{x}_0 = \hat{x}_0, \quad \bar{x}_1 = \hat{x}_1,$$

together with the centered linear Schrödinger bridge

$$(32) \quad d\tilde{x}_t = A_t \tilde{x}_t dt + B_t \tilde{u}_t(\tilde{x}_t) dt + D_t dw_t,$$

whose boundary distributions are the shifted Gaussian mixtures

$$\tilde{\rho}_0 := \sum_{i \in \mathcal{I}} \alpha_i^0 \mathcal{N}(m_i^0 - \hat{x}_0, \Sigma_i^0), \quad \tilde{\rho}_1 := \sum_{j \in \mathcal{J}} \alpha_j^1 \mathcal{N}(m_j^1 - \hat{x}_1, \Sigma_j^1).$$

The lifted construction can then be applied directly to this centered problem. Namely, for each source–target component pair (i, j) , one solves the Gaussian Schrödinger bridge, equivalently, the linear covariance-steering problem,

$$\mathcal{N}(m_i^0 - \hat{x}_0, \Sigma_i^0) \longrightarrow \mathcal{N}(m_j^1 - \hat{x}_1, \Sigma_j^1),$$

under the centered linear dynamics (32). Let the resulting pairwise law, density, drift, and kinetic cost be denoted by $\tilde{\mathbb{P}}^{ij}$, $\tilde{\rho}_t^{ij}$, \tilde{u}_t^{ij} , and C_{ij} , respectively. Given a component coupling $\pi \in \Pi(\alpha^0, \alpha^1)$, define the lifted centered law $\tilde{\mathbb{P}}_{\text{MF}}^\pi = \sum_{i \in \mathcal{I}} \sum_{j \in \mathcal{J}} \pi_{ij} \delta_{(i,j)} \otimes \tilde{\mathbb{P}}^{ij}$. Applying the same posterior-averaging construction used in (29)–(31), now to the centered variables, define the quantities

$$\tilde{\rho}_t^\pi(z) := \sum_{i \in \mathcal{I}} \sum_{j \in \mathcal{J}} \pi_{ij} \tilde{\rho}_t^{ij}(z), \quad \tilde{u}_t^\pi(z) := \sum_{i \in \mathcal{I}} \sum_{j \in \mathcal{J}} \tilde{\gamma}_{ij}(t, z) \tilde{u}_t^{ij}(z), \quad \tilde{\gamma}_{ij}(t, z) := \frac{\pi_{ij} \tilde{\rho}_t^{ij}(z)}{\tilde{\rho}_t^\pi(z)}.$$

The corresponding mean-field feedback in the original coordinates is then $u_t^\pi(x) = \bar{u}_t + \tilde{u}_t^\pi(x - \bar{x}_t)$, and the induced density is $\rho_t^\pi(x) = \tilde{\rho}_t^\pi(x - \bar{x}_t)$. Consequently, the unconstrained mean-field problem can be viewed as the composition of a deterministic mean-steering problem and a lifted centered Gaussian-mixture Schrödinger bridge. In this sense, the mixture-policy construction used for unconstrained mean-field Schrödinger bridges with Gaussian-mixture endpoints is precisely the projected Markov feedback associated with a component-labeled lifted path law.

§3.8. Hidden-label memory and Markovian projection. In this section, we distinguish the projected path law \mathbb{Q}^π in (21) and the Markov law generated by the posterior-averaged feedback \bar{u}^π in (31). The former is obtained by forgetting the auxiliary label in the lifted law, whereas the latter is obtained by driving the Brownian diffusion with the state-feedback drift \bar{u}^π . We denote by $\widehat{\mathbb{Q}}^\pi \in \mathcal{P}(\Omega)$ the path law induced by

$$dx_t = \bar{u}_t^\pi(x_t) dt + \sqrt{\varepsilon} dw_t, \quad x_0 \sim \rho_0.$$

By Corollary 1, this law is well defined, has finite kinetic energy, and satisfies $\text{Law}_{\widehat{\mathbb{Q}}^\pi}(x_t) = \rho_t^\pi(x) dx$ for $t \in [0, 1]$. On the other hand, \mathbb{Q}^π is generally a mixture of bridge laws with a hidden source–target label fixed for the whole trajectory. Therefore, even though each \mathbb{P}^{ij} is Markov, the mixture \mathbb{Q}^π need not be Markov with respect to the observed state process. To this end, let

$$(33) \quad \mathcal{F}_t^x := \sigma(x_s : 0 \leq s \leq t),$$

denote the observed state filtration. Under the lifted law $\tilde{\mathbb{P}}^\pi$, define the pathwise posterior label probabilities $\Gamma_{ij}^\pi(t) := \tilde{\mathbb{P}}^\pi(Z = (i, j) \mid \mathcal{F}_t^x)$. This should be distinguished from γ_{ij}^π in (30). The former conditions on the whole observed trajectory up to time t , whereas the latter conditions only on the current state. Define the \mathcal{F}_t^x -adapted [Pro04, Chapter I, §1] hidden-label drift $b_t^\pi := \sum_{i,j} \Gamma_{ij}^\pi(t) u_t^{ij}(x_t)$. This drift is generally non-Markovian, because it may depend on the observed past through the posterior $\Gamma_{ij}^\pi(t)$.

Proposition 7 (Hidden-label drift and Markovian projection). *For every $\pi \in \Pi(\alpha^0, \alpha^1)$, under the projected path law $\mathbb{Q}^\pi = (\mathcal{P}_\Omega)_\# \tilde{\mathbb{P}}^\pi$, there exists an $(\mathcal{F}_t^x)_{t \in [0,1]}$ -Brownian motion \tilde{w} such that we have the semimartingale representation*

$$x_t = x_0 + \int_0^t b_s^\pi ds + \sqrt{\varepsilon} \tilde{w}_t \quad \text{for } t \in [0, 1].$$

Moreover, for a.e. $t \in [0, 1]$, the posterior-averaged drift is a version of the conditional expectation

$$\bar{u}_t^\pi(x) = \mathbb{E}^{\mathbb{Q}^\pi} [b_t^\pi \mid x_t = x],$$

for ρ_t^π -a.e. x . Consequently, \bar{u}^π is the $L^2(dt \otimes \mathbb{Q}^\pi)$ -orthogonal projection of the hidden-label drift b^π onto the class of feedbacks depending only on the current state, i.e.,

$$(34) \quad \bar{u}^\pi \in \arg \min_v \mathbb{E}^{\mathbb{Q}^\pi} \left[\int_0^1 \|b_t^\pi - v_t(x_t)\|^2 dt \right],$$

where the minimization is over measurable feedbacks $(t, x) \mapsto v_t(x)$ for which the expression is finite.

PROOF. Let $\mathcal{G}_t := \sigma(Z) \vee \mathcal{F}_t^x$ be the smallest sigma algebra containing both $\sigma(Z)$ and \mathcal{F}_t^x , where F_t^x as in (33). For notational convenience, define the labeled drift $u_t^Z(x_t) := u_t^{ij}(x_t)$ on the event $\{Z = (i, j)\}$. Under $\bar{\mathbb{P}}^\pi$, conditional on $Z = (i, j)$, the canonical process has law \mathbb{P}^{ij} . Hence, in the enlarged filtration \mathcal{G}_t , the process $M_t := x_t - x_0 - \int_0^t u_s^Z(x_s) ds$ is a continuous $\bar{\mathbb{P}}^\pi$ -local martingale with quadratic variation $\langle M \rangle_t = \varepsilon t I_d$. This is the standard semimartingale decomposition of a diffusion in its natural enlarged filtration; see [Pro04, Chapter II, §1 and §6] and [KS91, Chapter 3, §2–4].

Define the optional projection [Pro04, Chapter 7], [LS01, Chapter 10], [BC09, Chapter 2] of the labeled drift onto the observed filtration by

$$b_t^\pi := \mathbb{E}^{\bar{\mathbb{P}}^\pi} \left[u_t^Z(x_t) \mid \mathcal{F}_t^x \right] = \sum_{i \in \mathcal{J}} \sum_{j \in \mathcal{J}} \bar{\mathbb{P}}^\pi(Z = (i, j) \mid \mathcal{F}_t^x) u_t^{ij}(x_t).$$

We next verify that b_t^π is indeed the drift of the projected process with respect to (\mathcal{F}_t^x) . Define

$$\tilde{M}_t := x_t - x_0 - \int_0^t b_s^\pi ds.$$

Let $0 \leq s \leq t$ and $A \in \mathcal{F}_s^x$. Since $A \in \mathcal{G}_s$, the (\mathcal{G}_t) -local martingale property of M , after localization if necessary, yields

$$\mathbb{E}^{\bar{\mathbb{P}}^\pi} \left[\mathbf{1}_A \left(x_t - x_s - \int_s^t u_r^Z(x_r) dr \right) \right] = 0.$$

Moreover, by the definition of b_r^π as the conditional expectation of $u_r^Z(x_r)$ given \mathcal{F}_r^x , and since $A \in \mathcal{F}_s^x \subseteq \mathcal{F}_r^x$ for $r \in [s, t]$, Fubini's theorem [Fol99, Theorem 2.37] and the tower property of expectation give

$$\mathbb{E}^{\bar{\mathbb{P}}^\pi} \left[\mathbf{1}_A \int_s^t u_r^Z(x_r) dr \right] = \mathbb{E}^{\bar{\mathbb{P}}^\pi} \left[\mathbf{1}_A \int_s^t b_r^\pi dr \right].$$

Therefore, $\mathbb{E}^{\bar{\mathbb{P}}^\pi} [\mathbf{1}_A (\tilde{M}_t - \tilde{M}_s)] = 0$. Hence, \tilde{M} is an (\mathcal{F}_t^x) -local martingale under the projected law \mathbb{Q}^π . Consequently,

$$x_t = x_0 + \int_0^t b_s^\pi ds + \tilde{M}_t,$$

is the (\mathcal{F}_t^x) -semimartingale decomposition of the projected process.

Since \tilde{M} differs from x only by a finite-variation process, subtracting the drift term does not change quadratic variation. Moreover, under each conditional law \mathbb{P}^{ij} , the coordinate process has diffusion coefficient $\sqrt{\varepsilon} I_d$. Hence, under the projected law \mathbb{Q}^π , the matrix-valued quadratic variation of the continuous local martingale \tilde{M} is $\langle \tilde{M} \rangle_t = \varepsilon t I_d$ for all $t \in [0, 1]$; see [Pro04, Chapter II, §6]. Therefore, by the multidimensional Lévy characterization of Brownian motion, there exists an (\mathcal{F}_t^x) -Brownian motion $(\tilde{w}_t)_{t \in [0, 1]}$ under \mathbb{Q}^π such that $\tilde{M}_t = \sqrt{\varepsilon} \tilde{w}_t$; see [KS91, Chapter 3, §3] or [RY99, Chapter IV, §3]. Thus,

$$(35) \quad dx_t = b_t^\pi dt + \sqrt{\varepsilon} d\tilde{w}_t,$$

with respect to the observed filtration (\mathcal{F}_t^x) .

We now identify the Markov projection of the adapted hidden-label drift b_t^π appearing in (35). Since \mathbf{Q}^π is the path-space marginal of $\bar{\mathbf{P}}^\pi$, conditional expectations of path-measurable quantities may be computed under $\bar{\mathbf{P}}^\pi$. Using the tower property:

$$\mathbb{E}^{\mathbf{Q}^\pi} [b_t^\pi | x_t = x] = \mathbb{E}^{\bar{\mathbf{P}}^\pi} \left[\mathbb{E}^{\bar{\mathbf{P}}^\pi} [u_t^Z(x_t) | \mathcal{F}_t^x] | x_t = x \right] = \mathbb{E}^{\bar{\mathbf{P}}^\pi} [u_t^Z(x_t) | x_t = x].$$

By the definition of the posterior weights, $\bar{\mathbf{P}}^\pi(Z = (i, j) | x_t = x) = \gamma_{ij}^\pi(t, x)$. Therefore,

$$\mathbb{E}^{\mathbf{Q}^\pi} [b_t^\pi | x_t = x] = \sum_{i \in \mathcal{I}} \sum_{j \in \mathcal{J}} \gamma_{ij}^\pi(t, x) u_t^{ij}(x) = \bar{u}_t^\pi(x).$$

Finally, the variational characterization (34) follows from the conditional-expectation projection theorem in L^2 : among all square-integrable feedbacks $v_t(x_t)$, the unique L^2 -orthogonal projection of b_t^π onto the closed subspace of functions measurable with respect to x_t is $\mathbb{E}^{\mathbf{Q}^\pi} [b_t^\pi | x_t] = \bar{u}_t^\pi(x_t)$. See, for example, [KS91, Ch. 1, Sec. 2], [ABG11, Bor05]. This proves the result. \square

Proposition 7 clarifies the status of the posterior-averaged feedback. As emphasized before, it is *not* introduced as an independent ansatz. Rather, it is the *Markovian projection*, in the conditional-expectation sense, of the non-Markov hidden-label drift associated with \mathbf{Q}^π . Thus, the state-feedback \bar{u}^π is obtained by replacing the full path-posterior label information $\Gamma_{ij}^\pi(t)$ with the current-state posterior $\gamma_{ij}^\pi(t, x_t)$. We now state the final result of this article.

Theorem 3 (Entropy decomposition through Markovization). *Recall that $\mathbf{Q}^\pi = (\mathcal{P}_\Omega)_\# \bar{\mathbf{P}}^\pi$, and let $\hat{\mathbf{Q}}^\pi$ be the Markov path law generated by \bar{u}^π . Then,*

$$(36) \quad \varepsilon \text{D}_{\text{KL}}(\mathbf{Q}^\pi \| \mathbf{R}^{\rho_0}) = \varepsilon \text{D}_{\text{KL}}(\hat{\mathbf{Q}}^\pi \| \mathbf{R}^{\rho_0}) + \varepsilon \text{D}_{\text{KL}}(\mathbf{Q}^\pi \| \hat{\mathbf{Q}}^\pi).$$

Moreover,

$$\varepsilon \text{D}_{\text{KL}}(\mathbf{Q}^\pi \| \hat{\mathbf{Q}}^\pi) = \frac{1}{2} \mathbb{E}^{\mathbf{Q}^\pi} \left[\int_0^1 \|b_t^\pi - \bar{u}_t^\pi(x_t)\|^2 dt \right].$$

Combining this with the projection-gap identity from §3.5 gives the three-level decomposition

$$(37) \quad \varepsilon \text{D}_{\text{KL}}(\bar{\mathbf{P}}^\pi \| \bar{\mathbf{R}}^\eta) = \varepsilon \text{D}_{\text{KL}}(\hat{\mathbf{Q}}^\pi \| \mathbf{R}^{\rho_0}) + \varepsilon \text{D}_{\text{KL}}(\mathbf{Q}^\pi \| \hat{\mathbf{Q}}^\pi) + \varepsilon \mathcal{G}(\pi, \eta).$$

PROOF. We first state the absolute continuity and integrability facts needed for the applications of Girsanov's theorem [KS91, Chapter 3, §3.5]. Since $\mathbf{Q}^\pi = \sum_{i \in \mathcal{I}} \sum_{j \in \mathcal{J}} \pi_{ij} \mathbf{P}^{ij}$ and $\mathbf{R}^{\rho_0} = \sum_{i \in \mathcal{I}} \alpha_i^0 \mathbf{R}^i$, and $\alpha_i^0 > 0$ for all $i \in \mathcal{I}$, every \mathbf{R}^{ρ_0} -null set is an \mathbf{R}^i -null set for each $i \in \mathcal{I}$. Since $\mathbf{P}^{ij} \ll \mathbf{R}^i$, it follows that $\mathbf{Q}^\pi \ll \mathbf{R}^{\rho_0}$. Furthermore, under the lifted law $\bar{\mathbf{P}}^\pi$, conditioned on $Z = (i, j)$, the path law is \mathbf{P}^{ij} . Hence,

$$(38) \quad \mathbb{E}^{\bar{\mathbf{P}}^\pi} \left[\int_0^1 \|u_t^Z(x_t)\|^2 dt \right] = \sum_{i \in \mathcal{I}} \sum_{j \in \mathcal{J}} \pi_{ij} \mathbb{E}^{\mathbf{P}^{ij}} \left[\int_0^1 \|u_t^{ij}(x_t)\|^2 dt \right] = 2 \sum_{i \in \mathcal{I}} \sum_{j \in \mathcal{J}} \pi_{ij} C_{ij} < +\infty.$$

By Proposition 7, $b_t^\pi = \mathbb{E}^{\bar{\mathbf{P}}^\pi} [u_t^Z(x_t) | \mathcal{F}_t^x]$. Therefore, Jensen's inequality gives

$$(39) \quad \mathbb{E}^{\mathbf{Q}^\pi} \left[\int_0^1 \|b_t^\pi\|^2 dt \right] \leq \mathbb{E}^{\bar{\mathbf{P}}^\pi} \left[\int_0^1 \|u_t^Z(x_t)\|^2 dt \right] < +\infty.$$

Thus, \mathbb{Q}^π has adapted drift b_t^π relative to the Brownian reference \mathbb{R}^{ρ_0} , with finite energy. From the finite-energy form of Girsanov's theorem, we have that

$$(40) \quad \varepsilon \mathbb{D}_{\text{KL}}(\mathbb{Q}^\pi \| \mathbb{R}^{\rho_0}) = \frac{1}{2} \mathbb{E}^{\mathbb{Q}^\pi} \left[\int_0^1 \|b_t^\pi\|^2 dt \right].$$

Similarly, since $\widehat{\mathbb{Q}}^\pi$ is the law of the Markov diffusion $dx_t = \bar{u}_t^\pi(x_t) dt + \sqrt{\varepsilon} dw_t$ with $x_0 \sim \rho_0$, and the corresponding Markov feedback has finite quadratic energy, another application of the finite-energy form of Girsanov's theorem gives

$$(41) \quad \varepsilon \mathbb{D}_{\text{KL}}(\widehat{\mathbb{Q}}^\pi \| \mathbb{R}^{\rho_0}) = \frac{1}{2} \mathbb{E}^{\widehat{\mathbb{Q}}^\pi} \left[\int_0^1 \|\bar{u}_t^\pi(x_t)\|^2 dt \right].$$

Since both $\widehat{\mathbb{Q}}^\pi$ and \mathbb{Q}^π have one-time marginals ρ_t^π , we obtain

$$(42) \quad \begin{aligned} \varepsilon \mathbb{D}_{\text{KL}}(\widehat{\mathbb{Q}}^\pi \| \mathbb{R}^{\rho_0}) &= \frac{1}{2} \mathbb{E}^{\widehat{\mathbb{Q}}^\pi} \left[\int_0^1 \|\bar{u}_t^\pi(x_t)\|^2 dt \right] = \int_0^1 \int_{\mathbb{R}^d} \frac{1}{2} \rho_t^\pi(x) \|\bar{u}_t^\pi(x)\|^2 dx dt \\ &= \frac{1}{2} \mathbb{E}^{\mathbb{Q}^\pi} \left[\int_0^1 \|\bar{u}_t^\pi(x_t)\|^2 dt \right]. \end{aligned}$$

We now compare \mathbb{Q}^π and $\widehat{\mathbb{Q}}^\pi$. Under \mathbb{Q}^π , the adapted drift is b_t^π , while under $\widehat{\mathbb{Q}}^\pi$, the adapted drift is $\bar{u}_t^\pi(x_t)$. The two laws have the same initial law and the same nondegenerate diffusion coefficient. Moreover, the energy identities (41) and (42) imply

$$(43) \quad \mathbb{E}^{\mathbb{Q}^\pi} \left[\int_0^1 \|b_t^\pi - \bar{u}_t^\pi(x_t)\|^2 dt \right] < +\infty,$$

because $\|b_t^\pi - \bar{u}_t^\pi(x_t)\|^2 \leq 2\|b_t^\pi\|^2 + 2\|\bar{u}_t^\pi(x_t)\|^2$, and the two terms on the right-hand side are integrable under \mathbb{Q}^π by (41) and (42), respectively. The finite-energy estimate (43) implies, by Girsanov's theorem, that $\mathbb{Q}^\pi \ll \widehat{\mathbb{Q}}^\pi$. Therefore, the standard finite-energy relative-entropy formula [KS91, Chapter 3, Section 5] for two diffusion laws with the same initial law and the same nondegenerate diffusion coefficient gives

$$(44) \quad \varepsilon \mathbb{D}_{\text{KL}}(\mathbb{Q}^\pi \| \widehat{\mathbb{Q}}^\pi) = \frac{1}{2} \mathbb{E}^{\mathbb{Q}^\pi} \left[\int_0^1 \|b_t^\pi - \bar{u}_t^\pi(x_t)\|^2 dt \right].$$

Finally, we show the first decomposition (36). By Proposition 7, $\bar{u}_t^\pi(x_t) = \mathbb{E}^{\mathbb{Q}^\pi} [b_t^\pi | x_t]$. Hence, the orthogonality property of conditional expectation gives, for a.e. $t \in [0, 1]$,

$$(45) \quad \mathbb{E}^{\mathbb{Q}^\pi} [(b_t^\pi - \bar{u}_t^\pi(x_t)) \cdot \bar{u}_t^\pi(x_t)] = 0.$$

Consequently, we have $\mathbb{E}^{\mathbb{Q}^\pi} \|b_t^\pi\|^2 = \mathbb{E}^{\mathbb{Q}^\pi} \|\bar{u}_t^\pi(x_t)\|^2 + \mathbb{E}^{\mathbb{Q}^\pi} \|b_t^\pi - \bar{u}_t^\pi(x_t)\|^2$, for a.e. $t \in [0, 1]$. Integrating with respect to time and using the three relative-entropy identities (41)–(43) gives

$$(46) \quad \varepsilon \mathbb{D}_{\text{KL}}(\mathbb{Q}^\pi \| \mathbb{R}^{\rho_0}) = \varepsilon \mathbb{D}_{\text{KL}}(\widehat{\mathbb{Q}}^\pi \| \mathbb{R}^{\rho_0}) + \varepsilon \mathbb{D}_{\text{KL}}(\mathbb{Q}^\pi \| \widehat{\mathbb{Q}}^\pi).$$

Finally, the projection-gap identity from §3.5 gives

$$(47) \quad \varepsilon \mathbb{D}_{\text{KL}}(\bar{\mathbb{P}}^\pi \| \bar{\mathbb{R}}^\eta) = \varepsilon \mathbb{D}_{\text{KL}}(\mathbb{Q}^\pi \| \mathbb{R}^{\rho_0}) + \varepsilon \mathcal{G}(\pi, \eta).$$

Using the Markovization identity (46) into the scaled projection-gap identity (47) yields the desired result (37). \square

Remark 6 (When does the Markovization loss vanish?). *The term $\mathbb{D}_{\text{KL}}(\mathbb{Q}^\pi \| \widehat{\mathbb{Q}}^\pi)$ vanishes if and only if $\mathbb{Q}^\pi = \widehat{\mathbb{Q}}^\pi$. By the Girsanov representation above, this is equivalent to $b_t^\pi = \bar{u}_t^\pi(x_t)$ for $dt \otimes \mathbb{Q}^\pi$ -a.e. (t, ω) . In other words, the hidden-label drift must already be determined by the current state, i.e., the additional label information contained in the observed past path must not improve the prediction of the current drift beyond what is already known from x_t . The condition $b_t^\pi = \bar{u}_t^\pi(x_t)$ for $dt \otimes \mathbb{Q}^\pi$ -a.e. (t, ω) , fails, in*

general, because the past trajectory may contain information about which component pair (i, j) was selected, and this information is not usually contained in the current state alone. Thus, \mathbf{Q}^π is generally non-Markov, whereas $\widehat{\mathbf{Q}}^\pi$ is Markov by construction. The condition can, nevertheless, hold in useful cases. For example, if all active pairwise bridges have the same feedback drift, say $x \mapsto u_t^{ij}(x) := u_t^\circ(x)$ for all $(i, j) \in \text{supp } \pi$, then both the hidden-label drift b_t^π and the posterior-averaged drift $\bar{u}_t^\pi(x_t)$ reduce to $u_t^\circ(x_t)$, independently of the posterior label probabilities, and hence $D_{\text{KL}}(\mathbf{Q}^\pi \| \widehat{\mathbf{Q}}^\pi) = 0$. This situation includes, for instance, a common open-loop feedforward steering law $x \mapsto u_t^{ij}(x) := v_t$ for all active pairs, identical affine covariance-steering feedbacks $x \mapsto u_t^{ij}(x) := A_t x + c_t$, a rigid translation of all active Gaussian components by the same displacement vector, or a symmetric multi-agent formation-control setting in which several label assignments induce the same instantaneous averaged velocity field.

§4. Numerical experiments

In this section, we present several numerical examples to illustrate that the lifted formulation helps in three concrete ways: **(a)** it reduces the continuous multimodal steering problem to closed-form Gaussian component bridges together with the finite-dimensional coupling problem (18); **(b)** it produces an explicit projected Markov feedback through (29)–(31); **(c)** it exposes the component-level assignment structure through the optimized coupling π^\star , which is not directly visible in a grid-based unlabeled Schrödinger bridge computation. The lifting gives the following structured computational recipe:³

$$(p_i^0, p_j^1) \mapsto (P^{ij}, C_{ij}) \implies C_{ij} \mapsto \pi^\star \implies (\pi^\star, P^{ij}) \mapsto (\rho_t^{\pi^\star}(\cdot), \bar{u}_t^{\pi^\star}(\cdot)).$$

§ 4.1. A one-dimensional mixture-to-mixture example. We first consider a one-dimensional example in order to illustrate the lifted construction, the optimized component coupling, and the projected Markov drift. We take $\varepsilon = 0.35$ and prescribe the initial and terminal Gaussian mixtures

$$\rho_0 := 0.65 \mathcal{N}(-3, 0.45^2) + 0.35 \mathcal{N}(2, 0.60^2),$$

and

$$\rho_1 := 0.35 \mathcal{N}(-1.5, 0.55^2) + 0.65 \mathcal{N}(3.5, 0.45^2).$$

Thus $N_1 = N_2 = 2$, with mixture weights $\alpha^0 := (0.65, 0.35)^\top$ and $\alpha^1 := (0.35, 0.65)^\top$. The endpoint densities are shown in Figure 2a. Notice that the initial distribution has more mass in its left component, while the terminal distribution has more mass in its right component. Therefore, any feasible mixture-to-mixture steering must split part of the left initial component and send it to the right terminal component. For each component pair (i, j) , we compute the pairwise Gaussian Schrödinger bridge using Proposition 2. The resulting kinetic-energy costs C_{ij} , was found to be

$$[C_{ij}]_{(i,j)} := C = \begin{pmatrix} 1.1545 & 21.1967 \\ 6.1869 & 1.2415 \end{pmatrix}.$$

As expected, the diagonal assignments are energetically cheap, whereas the assignment from the left initial component to the right terminal component has a high cost, and the assignment from the right initial component to the left terminal component is also relatively expensive.

³All numerical simulations were performed in MATLAB R2022a on the first author's 2021 MacBook Pro with an Apple M1 processor.

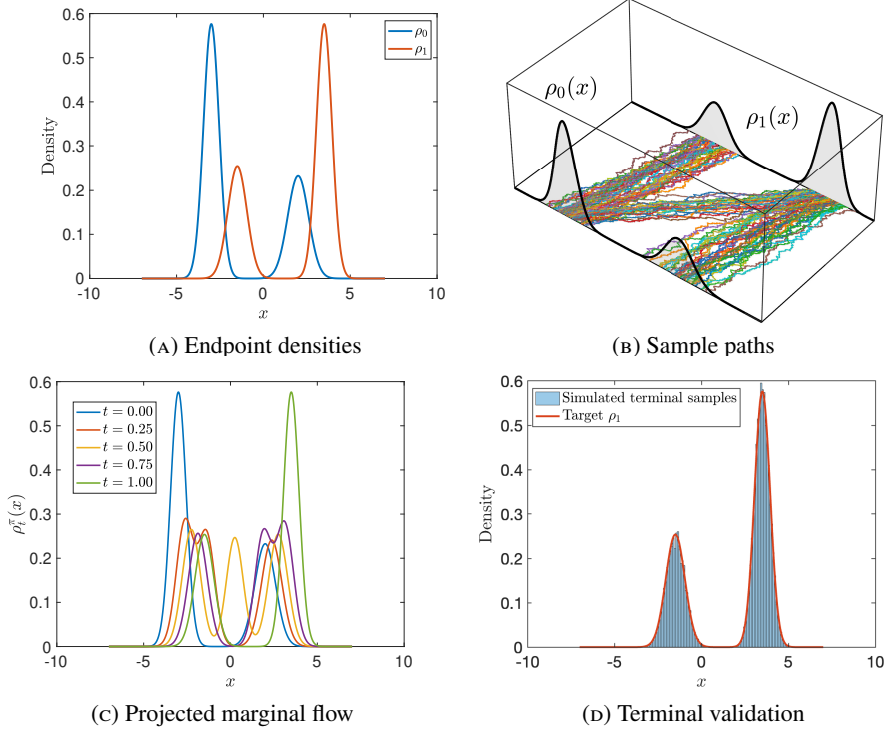


FIGURE 2. One-dimensional Gaussian-mixture Schrödinger bridge experiment.

We choose the prior coupling to be $\eta_{ij}^{\text{prod}} := \alpha_i^0 \alpha_j^1$. Solving the lifted finite-dimensional problem by Sinkhorn scaling (with 100 Sinkhorn iterations) yields

$$\pi^* = \begin{pmatrix} 0.35 & 0.30 \\ 0 & 0.35 \end{pmatrix},$$

where entries below 10^{-5} are displayed as zero. The row and column sums satisfy $\sum_j \pi_{ij}^* = \alpha_i^0$, and $\sum_i \pi_{ij}^* = \alpha_j^1$, as required. The interpretation is clear: the first initial component has mass 0.65, but the first terminal component requires only mass 0.35. Hence, approximately 0.35 units of mass are assigned from component 1 to component 1, while the remaining 0.30 units are assigned from component 1 to component 2. The second initial component is assigned almost entirely to the second terminal component.

Given π^* , the lifted marginal flow is $x \mapsto \rho_t^{\pi^*}(x) = \sum_{i,j} \pi_{ij}^* \rho_t^{ij}(x)$. The projected Markov drift is then defined by posterior averaging $x \mapsto \bar{u}_t^{\pi^*}(x) = \sum_{i,j} \gamma_{ij}^{\pi^*}(t, x) u_t^{ij}(x)$, with $\gamma_{ij}^{\pi^*}(t, x) = \pi_{ij}^* \rho_t^{ij}(x) / \rho_t^{\pi^*}(x)$. Figure 2c shows the analytic density flow $\rho_t^{\pi^*}$ at several slices of times. The plot confirms the endpoint identities $\rho_0^{\pi^*} = \rho_0$, and $\rho_1^{\pi^*} = \rho_1$, which are guaranteed by Proposition 3. The intermediate densities reveal the three dominant transport channels corresponding to the non-negligible entries of π^* : mass from component 1 to component 1, mass from component 1 to component 2, and mass from component 2 to component 2. The missing channel from component 2 to component 1 is consistent with the zero value of π_{21}^* .

To verify the projected drift construction, we simulated the Markov diffusion $dx_t = \bar{u}_t^{\pi^*}(x_t) dt + \sqrt{\varepsilon} dw_t$, with $x_0 \sim \rho_0$ using 800 Euler-Maruyama steps. The resulting sample paths are shown in Figure 2b. The trajectories visibly split into the same three

channels identified by the optimized coupling. In particular, a portion of the left initial component moves to the left terminal component, another portion moves to the right terminal component, and the right initial component moves primarily to the right terminal component. This provides a trajectory-level visualization of the Markovized marginal flow induced by the coupling matrix π^\star . Figure 2d compares the terminal empirical distribution obtained by simulating the projected drift with the prescribed target density ρ_1 . The close agreement verifies numerically that the projected drift generates the desired terminal marginal. This is the simulation-level counterpart of the Fokker–Planck feasibility statement proved in Proposition 6.

We also compared our lifted construction with a direct numerical approximation of the unlabeled Schrödinger bridge for the same one-dimensional Gaussian-mixture endpoints. The direct method discretizes the one-dimensional state space. Specifically, it first chooses a bounded computational interval $D := [y_{\min}, y_{\max}] \subset \mathbb{R}$ containing the effective support of the endpoint densities ρ_0 and ρ_1 , and then introduces a uniform spatial grid $\{y_k\}_{k=1}^M \subset D$. The continuous endpoint densities ρ_0 and ρ_1 are then replaced by normalized probability vectors $r_0, r_1 \in \Delta_M$, obtained by evaluating/integrating the densities over the grid cells. With $K_{k\ell}$ denoting the Brownian heat kernel between grid points y_k and y_ℓ , the method solves the finite-dimensional entropy-projection problem

$$\min_{\Gamma \in \Pi(r_0, r_1)} \sum_{k, \ell} \Gamma_{k\ell} \log \frac{\Gamma_{k\ell}}{K_{k\ell}},$$

using Sinkhorn scaling, following the Schrödinger–Fortet–Sinkhorn viewpoint [CGP21]. We found that the direct-SB energy, in the same kinetic-energy scaling used throughout the paper, is $J_{\text{direct}} = 6.231$. or 100 Sinkhorn iterations, the marginal residuals were $\|\gamma \mathbf{1} - r_0\|_1 = 4 \times 10^{-13}$, and $\|\gamma^\top \mathbf{1} - r_1\|_1 = 6 \times 10^{-14}$, where r_0, r_1 are the discretized endpoint marginals and γ is the computed endpoint coupling. This means that, among all state-space controlled diffusions steering the full mixture ρ_0 to the full mixture ρ_1 , the minimum energy is approximately 6.231.

Using the projected density $\rho_t^{\pi^\star}(\cdot)$ and the feedback $\bar{u}_t^{\pi^\star}(\cdot)$, we have

$$J_{\text{proj}} := \int_0^1 \int_{\mathbb{R}} \frac{1}{2} \rho_t^{\pi^\star}(x) |\bar{u}_t^{\pi^\star}(x)|^2 dx dt,$$

which numerically is $J_{\text{proj}} = 6.437$. The relative gap is

$$\frac{J_{\text{proj}} - J_{\text{direct}}}{J_{\text{direct}}} = \frac{0.2061072060}{6.2313514143} \approx 0.03308.$$

Thus, the advantage of our method should be understood as follows: it provides an explicit, structured, low-dimensional, interpretable, feedback-realizable construction. The direct numerical Schrödinger bridge is a grid-based reference method. In one dimension, it is easy to implement. However, in dimension d , if one uses M grid points per coordinate, the endpoint grid has M^d points, and the endpoint coupling matrix has roughly $M^d \times M^d = M^{2d}$ entries. Thus, even a moderately fine two- or three-dimensional grid becomes expensive quickly. Our approach replaces this massive endpoint coupling by a component coupling of size $N_1 \times N_2$; see Table 1 for details.

§ 4.2. Two-dimensional examples. We next consider two-dimensional Gaussian-mixture examples. We provide three illustrations. First, an example where both endpoint distributions are mixtures with three components. We will see that the optimized coupling $\pi^\star \in \Pi(\alpha^0, \alpha^1)$ is nontrivial. That is, it has to decide how much mass from each source component goes to each target component, balancing pairwise costs C_{ij} against the entropy term. The second example, has only one source component. Thus, it verifies

TABLE 1. Numerical statistics. The computation time (in secs) is median run times over 30 repetitions.

Method	Size	Energy	Time
Direct SB	601×601	6.231	4.4×10^{-1}
Ours	2×2	6.437	4.4×10^{-4}

our developments with intuitive numerical visualizations. The final example illustrates the developments through a shape-transformation example.

§ 4.2.1. *Example 1.* We take $d = 2$, terminal time $T = 1$, and diffusion parameter $\varepsilon = 0.3$. The initial and terminal distributions are three-component Gaussian mixtures

$$x \mapsto \rho_0(x) := \sum_{i=1}^3 \alpha_i^0 \mathcal{N}(x; m_i^0, \Sigma_i^0), \quad x \mapsto \rho_1(x) := \sum_{j=1}^3 \alpha_j^1 \mathcal{N}(x; m_j^1, \Sigma_j^1),$$

with mixture weights $\alpha^0 := (0.40, 0.35, 0.25)^\top$, $\alpha^1 := (0.25, 0.45, 0.30)^\top$. The component means are $m_1^0 := (-4, -2)$, $m_2^0 := (-4, 1.8)$, and $m_3^0 := (-1, 0)$, and $m_1^1 := (2.5, -2.5)$, $m_2^1 := (4, 0.4)$, and $m_3^1 := (2.5, 2.7)$. The covariance matrices are

$$\Sigma_1^0 := \begin{pmatrix} 0.35 & 0.08 \\ 0.08 & 0.28 \end{pmatrix}, \quad \Sigma_2^0 := \begin{pmatrix} 0.30 & -0.06 \\ -0.06 & 0.45 \end{pmatrix}, \quad \Sigma_3^0 := \begin{pmatrix} 0.48 & 0 \\ 0 & 0.35 \end{pmatrix},$$

and

$$\Sigma_1^1 := \begin{pmatrix} 0.40 & -0.05 \\ -0.05 & 0.30 \end{pmatrix}, \quad \Sigma_2^1 := \begin{pmatrix} 0.35 & 0.07 \\ 0.07 & 0.42 \end{pmatrix}, \quad \Sigma_3^1 := \begin{pmatrix} 0.32 & -0.04 \\ -0.04 & 0.36 \end{pmatrix}.$$

For each pair (i, j) , we compute the pairwise Gaussian Schrödinger bridge from the initial component $\mathcal{N}(m_i^0, \Sigma_i^0)$ to the terminal component $\mathcal{N}(m_j^1, \Sigma_j^1)$. The corresponding kinetic cost is

$$C \approx \begin{pmatrix} 21.31 & 34.92 & 32.24 \\ 30.45 & 33.05 & 21.61 \\ 9.34 & 12.66 & 9.87 \end{pmatrix}.$$

For this example, the third initial component has comparatively low transport cost to all terminal components, especially to the first and third terminal components. By contrast, transporting the first initial component to the second or third terminal component and the second initial component to the first or second terminal component are substantially more expensive.

We choose the prior coupling to be the independent coupling $\eta_{ij} = \alpha_i^0 \alpha_j^1$ and solved the finite-dimensional lifted problem by Sinkhorn scaling to obtain π^* , as follows

$$\pi^* \approx \begin{pmatrix} 0.25 & 0.15 & 0 \\ 0 & 0.05 & 0.30 \\ 0 & 0.25 & 0 \end{pmatrix},$$

where entries below 10^{-7} are displayed as zero. The row and column sums satisfy $\sum_j \pi_{ij}^* = \alpha_i^0$, $\sum_i \pi_{ij}^* = \alpha_j^1$. The transport contribution is approximately $\sum_{i,j} \pi_{ij}^* C_{ij} \approx 21.87$, and the discrete entropy term is approximately 0.659. Thus, the finite-dimensional lifted objective is approximately $\sum_{i,j} \pi_{ij}^* C_{ij} + \varepsilon \mathbf{D}_{\text{KL}}(\pi^* \|\eta) \approx 22.06$.

Given π^* , using the lifted marginal density $\rho_i^{\pi^*}$, and the projected Markov drift $\bar{u}_i^{\pi^*}$, we then simulated the Markov diffusion

$$dx_t = \bar{u}_i^{\pi^*}(x_t) dt + \sqrt{\varepsilon} dw_t, \quad x_0 \sim \rho_0.$$

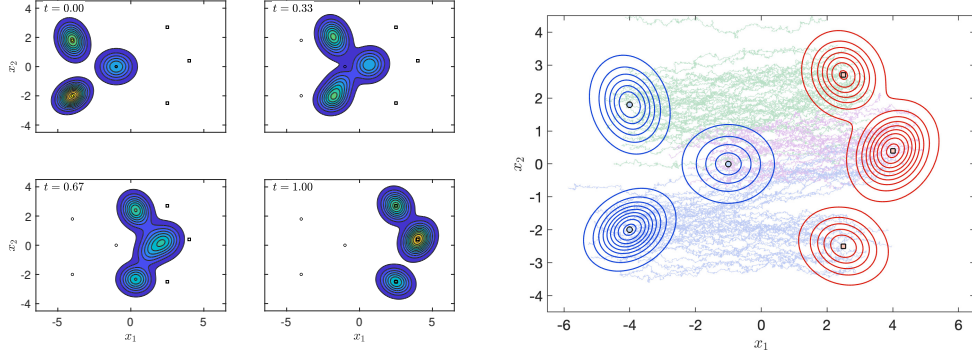


FIGURE 3. The evolution of the projected density $\rho_t^{\pi^*}(\cdot)$ at several time-slices (left subfigure) and sample paths of the Markov diffusion under Euler-Maruyama steps (right subfigure).

TABLE 2. Numerical statistics. The computation time (in secs) is the median run times over 20 repetitions.

Method	Size	Energy	Time
Direct SB	3111×3111	21.197	1.5
Ours	3×3	21.267	1.3×10^{-2}

In the simulation, 30,000 particles were propagated using 1,500 Euler–Maruyama steps, and 100 sample paths were retained for visualization.

The right-hand subfigure in Figure 3 shows sample paths generated by the projected Markov drift. The paths are colored according to their initial component, while the endpoint density contours are drawn on top. The figure illustrates the Eulerian projected-drift construction at the trajectory level. At the level of one-time marginals, the observed particle flow is consistent with the optimized coupling: density initially concentrated near each source component is transported toward the terminal regions favored by the large entries of π^* . The left-hand subfigure in Figure 3 shows the analytic projected density $\rho_t^{\pi^*}$ at four times, $t = 0, \frac{1}{3}, \frac{2}{3}$, and $t = 1$. The panel at $t = 0$ recovers the prescribed initial mixture ρ_0 , and the panel at $t = 1$ recovers the prescribed terminal mixture ρ_1 . The intermediate panels show the splitting and recombination of density induced by the optimized coupling. This figure provides a direct numerical verification of the theoretical endpoint identities $\rho_0^{\pi^*} = \rho_0$, and $\rho_1^{\pi^*} = \rho_1$. We also report similar numerical statistics as before; see Table 2.

§4.2.2. *Example 2: An eight-mode splitting.* We next present a two-dimensional radial example designed to visualize the projected Markov drift when a single unimodal initial distribution is steered to a highly multimodal terminal distribution. This example illustrates how the posterior-averaged projected drift splits one initial cloud into several terminal clusters. We take $d = 2, T = 1, \varepsilon = 0.08$. The initial distribution is a single Gaussian centered at the origin, $\rho_0(x) = \mathcal{N}(x; m_0, \Sigma_0)$, with $m_0 := (0, 0), \Sigma_0 := 0.15I_2$. The terminal distribution is an eight-component Gaussian mixture whose component means are arranged uniformly on a circle of radius $r = 5.1$, i.e., $x \mapsto \rho_1(x) := \frac{1}{8} \sum_{j=1}^8 \mathcal{N}(x; m_j^1, \Sigma_j^1)$, where

$$m_j^1 := r(\cos \theta_j, \sin \theta_j) \text{ and } \theta_j := \frac{2\pi(j-1)}{8} \text{ for } j = 1, \dots, 8.$$

The terminal covariance matrices are anisotropic with their major axes aligned with the radial directions. Specifically, if

$$R_j := \begin{pmatrix} \cos \theta_j & -\sin \theta_j \\ \sin \theta_j & \cos \theta_j \end{pmatrix}, \quad \text{then} \quad \Sigma_j^1 = R_j \begin{pmatrix} 0.16 & 0 \\ 0 & 0.10 \end{pmatrix} R_j^\top.$$

Thus, the terminal density consists of eight localized Gaussian modes distributed around a circle. We carried out all other numerical steps as before and thus omitted the details. The

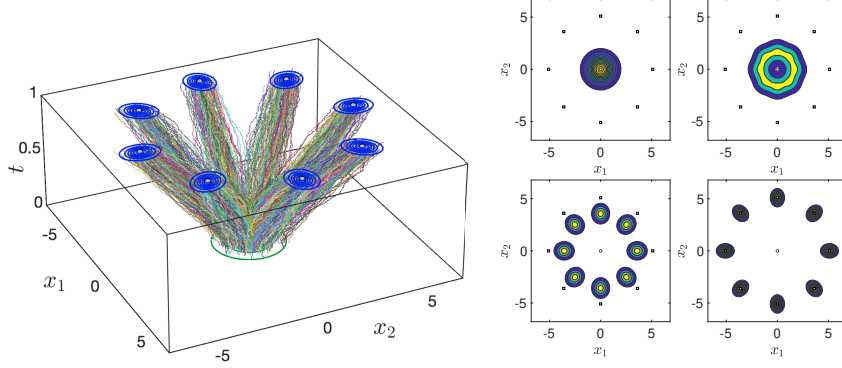


FIGURE 4. The evolution of the sample paths of the Markov diffusion under Euler-Maruyama steps (left subfigure) and the corresponding density evolution (right subfigure) at different time-slices.

left subfigure in Figure 4 shows a three-dimensional space-time visualization in (x_1, x_2, t) . The green contour lies in the plane $t = 0$, representing the initial Gaussian. The blue contours lie in the plane $t = 1$, representing the eight terminal Gaussian components. The right subfigure in Figure 4 shows the analytic projected density $\rho_t^{\pi^*} = \frac{1}{8} \sum_{j=1}^8 \rho_t^{1j}$ at several intermediate times. At $t = 0$, the density is the initial Gaussian at the origin. At $t = 1$, the density becomes the eight-component terminal mixture. The intermediate panels show how the initially unimodal density spreads and separates into multiple branches. This example demonstrates that the projected Markov drift is capable of producing a highly multimodal terminal distribution from a single unimodal initial distribution.

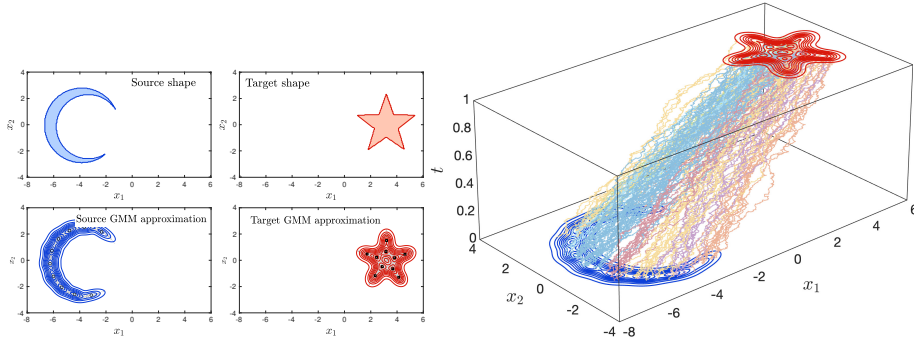


FIGURE 5. The crescent source and star target shapes and their GMM approximations (left subfigure). The sample paths of the Markov diffusion under Euler-Maruyama steps (right subfigure).

§ 4.2.3. *Example 3 (Shape matching)*. As a final visual illustration, we consider an image-inspired density steering problem. A crescent-shaped source silhouette and a star-shaped target silhouette are first converted into point clouds, and each point cloud is

approximated by a finite Gaussian mixture; see Figure 5. More precisely, they were approximated by 10 Gaussian components with mixture weights as follows

$$\alpha^0 = (0.13, 0.05, 0.10, 0.07, 0.09, 0.13, 0.12, 0.12, 0.04, 0.10)^\top$$

$$\alpha^1 = (0.12, 0.07, 0.07, 0.11, 0.11, 0.12, 0.08, 0.09, 0.08, 0.12)^\top.$$

Our lifted construction is then applied to these fitted Gaussian-mixture endpoints. The right-hand subfigure in Figure 5 shows sample paths generated by the projected Markov drift \bar{u}^{π^*} , illustrating the stochastic transport from the source region to the target region. Figure 6 shows the corresponding analytic projected density evolution $x \mapsto \rho_t^{\pi^*}(x)$ which deforms the crescent-shaped density into the star-shaped density.

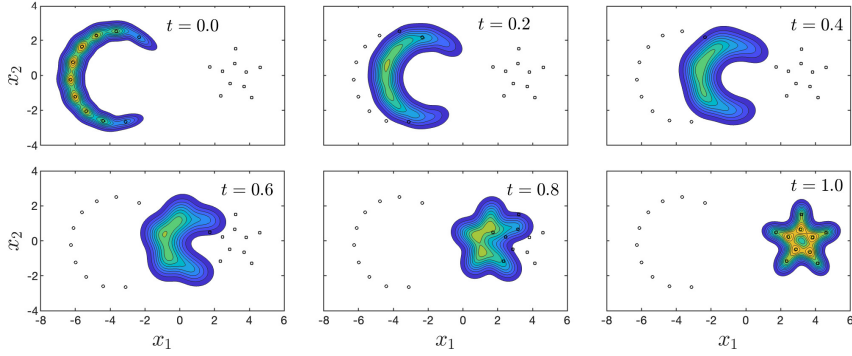


FIGURE 6. The evolution of the projected density $\rho_t^{\pi^*}(\cdot)$ for the shape matching problem.

To illustrate the role of the prior component coupling η (as discussed in Remark 5), we additionally perform a prior-sensitivity experiment for this example. We compare three admissible prior couplings η . The first is the neutral product prior $\eta^{\text{prod}} := \alpha^0(\alpha^1)^\top$ (as employed in the previous examples). The second is a diagonal-favoring prior, and the third is a rotated prior. Since the source and target weights are not uniform, the diagonal and rotated priors cannot be simple permutation matrices. Instead, we first construct two couplings $\tilde{\eta}^{\text{diag}}, \tilde{\eta}^{\text{rot}} \in \Pi(\alpha^0, \alpha^1)$, where $\tilde{\eta}^{\text{diag}}$ places as much mass as possible along the diagonal $i = j$, while $\tilde{\eta}^{\text{rot}}$ places as much mass as possible along the shifted diagonal $j = i + 3 \pmod{10}$. Any remaining mass is assigned greedily to satisfy the prescribed row and column sums. We then blend these structured couplings with the product prior to generate

$$\eta^{\text{diag}} := (1 - \theta)\eta^{\text{prod}} + \theta\tilde{\eta}^{\text{diag}}, \quad \eta^{\text{rot}} := (1 - \theta)\eta^{\text{prod}} + \theta\tilde{\eta}^{\text{rot}},$$

with $\theta = 0.90$. This blending guarantees strict positivity of all entries, while preserving the marginals α^0 and α^1 . For each choice $\eta \in \{\eta^{\text{prod}}, \eta^{\text{diag}}, \eta^{\text{rot}}\}$, we solve

$$\pi_\eta^* \in \arg \min_{\pi \in \Pi(\alpha^0, \alpha^1)} \left\{ \sum_{i,j} \pi_{ij} C_{ij} + \varepsilon \mathcal{D}_{\text{KL}}(\pi \| \eta) \right\}.$$

Figure 7 shows that the optimized component assignment depends visibly on the prior coupling. Consequently, as we discussed before, η is *not merely an interpretability device*, it acts as a modeling input in the lifted assignment layer.

§5. Concluding remarks

In this article, we developed a lifted Schrödinger bridge construction for Gaussian-mixture endpoint distributions by augmenting trajectories with source–target component

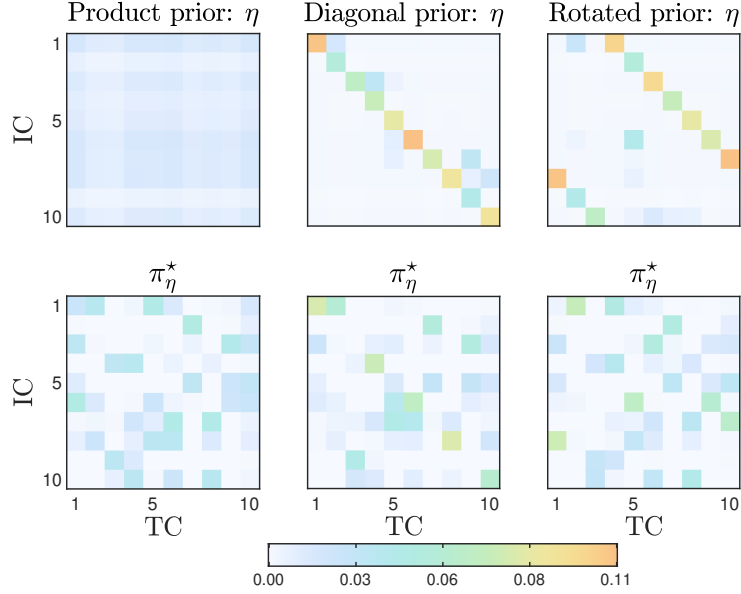


FIGURE 7. Effect of the prior component coupling in the shape-matching example. The top row shows the prescribed prior couplings η , and the bottom row shows the corresponding optimized couplings π_η^* . The product prior is neutral, the diagonal-favoring prior encourages $i \mapsto i$ assignments, and the rotated prior encourages the shifted assignment $j = i + 3 \pmod{10}$. All entries represent fractions of total mass assigned from an initial component to a terminal component. Here IC denotes initial component and TC denotes terminal component.

labels, thereby reducing the mixture-to-mixture problem to explicit Gaussian component bridges and a finite-dimensional entropic coupling problem. Projecting the lifted law back to the original state space yields a feasible feedback construction that matches the prescribed endpoints, admits a certified kinetic-energy upper bound, and is numerically shown to achieve performance very close to direct grid-based Schrödinger bridge solvers, while being numerically faster and retaining a much more interpretable and low-dimensional component-level structure.

Several extensions of this work are natural. First, the Brownian Gaussian component bridges can be replaced by linear-system covariance-steering bridges, or, more generally, by numerically computed nonlinear-prior Schrödinger bridges. In that case, the lifted architecture remains the same, but the component quantities $(\rho_i^{ij}, u_i^{ij}, C_{ij})$ are computed numerically rather than in closed form. Second, state constraints can be incorporated at the component level by replacing each pairwise bridge with a constrained Schrödinger bridge or chance-constrained covariance-steering subproblem; the finite-dimensional assignment layer is then preserved, while the costs C_{ij} encode constrained transfer geometry. Third, unconstrained linear mean-field Schrödinger bridges with Gaussian-mixture endpoints can be handled by combining deterministic mean steering with a lifted centered Gaussian-mixture bridge. Stochastic maximum principle [DEHA⁺24, DEDKC25, DEH26, Ela26], unbalanced optimal transport [CGP25, NGK26], and optimal stopping [SGPT26, EG25] based viewpoints would also be interesting. Finally, a sharper analysis of the projection gap between the lifted and unlabeled path laws would further clarify when the lifted construction is close to the true unlabeled optimum.

§6. Acknowledgment

During the preparation of this manuscript, the author(s) used OpenAI's ChatGPT to improve grammar and English usage and to assist in generating colored visualizations for some plots. The author(s) take full responsibility for all remaining errors.

§7. Appendix

PROOF OF PROPOSITION 2. Let $(x_t)_{t \in [0,1]}$ denote the canonical process under P^{ij} . Since P^{ij} is a Brownian reciprocal process with Gaussian endpoint law, conditional on (x_0, x_1) , the path is a Brownian bridge. Therefore, for every $t \in [0, 1]$, $x_t = (1-t)x_0 + tx_1 + \sqrt{\varepsilon} B_t^{\text{br}}$, where $(B_t^{\text{br}})_{t \in [0,1]}$ is a standard Brownian bridge, independent of (x_0, x_1) , satisfying $\mathbb{E}[B_t^{\text{br}}] = 0$, and $\text{Cov}(B_t^{\text{br}}) = t(1-t)I$. Taking expectations gives

$$\mathbb{E}[x_t] = (1-t)\mathbb{E}[x_0] + t\mathbb{E}[x_1] = (1-t)m_i^0 + tm_j^1,$$

which proves the formula for m_t^{ij} . Using independence of B_t^{br} from (x_0, x_1) and $\text{Cov}(x_0, x_1) = \Sigma_{01}^{ij}$, we obtain $\text{Cov}(x_t) = \text{Cov}((1-t)x_0 + tx_1) + \varepsilon \text{Cov}(B_t^{\text{br}})$. Hence,

$$\Sigma_t^{ij} = (1-t)^2 \Sigma_i^0 + t^2 \Sigma_j^1 + t(1-t)(\Sigma_{01}^{ij} + (\Sigma_{01}^{ij})^\top) + \varepsilon t(1-t)I,$$

as desired. In particular, $\Sigma_t^{ij} \in \mathbb{S}_{++}^d$ for every $t \in [0, 1]$, so $(\Sigma_t^{ij})^{-1}$ is well defined. Next, we derive the drift. For a Brownian bridge with random endpoints, the drift is [KS91, Chapter 5, Section 6]

$$u_t^{ij}(x) = \frac{1}{1-t} (\mathbb{E}[x_1 | x_t = x] - x) \quad \text{for } t \in [0, 1).$$

Since (x_t, x_1) is jointly Gaussian, the conditional expectation is affine, and thus, we get $\mathbb{E}[x_1 | x_t = x] = m_j^1 + \text{Cov}(x_1, x_t)(\Sigma_t^{ij})^{-1}(x - m_t^{ij})$. Moreover, $\text{Cov}(x_1, x_t) = (1-t)(\Sigma_{01}^{ij})^\top + t\Sigma_j^1$. Therefore,

$$u_t^{ij}(x) = \frac{m_j^1 - m_t^{ij}}{1-t} + \frac{\text{Cov}(x_1, x_t) - \Sigma_t^{ij}}{1-t} (\Sigma_t^{ij})^{-1} (x - m_t^{ij}).$$

Since $m_j^1 - m_t^{ij} = (1-t)(m_j^1 - m_i^0)$, the constant term becomes $c_{ij} = m_j^1 - m_i^0$. Also,

$$\text{Cov}(x_1, x_t) - \Sigma_t^{ij} = (1-t) \left((1-t)((\Sigma_{01}^{ij})^\top - \Sigma_i^0) + t(\Sigma_j^1 - \Sigma_{01}^{ij} - \varepsilon I) \right),$$

and hence,

$$\frac{\text{Cov}(x_1, x_t) - \Sigma_t^{ij}}{1-t} = (1-t) \left((\Sigma_{01}^{ij})^\top - \Sigma_i^0 \right) + t(\Sigma_j^1 - \Sigma_{01}^{ij} - \varepsilon I) = S_t^{ij}.$$

Thus, we have $u_t^{ij}(x) = S_t^{ij} (\Sigma_t^{ij})^{-1} (x - m_t^{ij}) + c_{ij}$, which proves the affine drift formula in Proposition (2-b).

Finally, by definition of the pairwise cost and the Girsanov identity, we have that

$$C_{ij} = \int_0^1 \int_{\mathbb{R}^d} \frac{1}{2} \rho_t^{ij}(x) \|u_t^{ij}(x)\|^2 dx dt.$$

Since under ρ_t^{ij} one has $x_t - m_t^{ij} \sim \mathcal{N}(0, \Sigma_t^{ij})$, and $u_t^{ij}(x) = A_t^{ij}(x_t - m_t^{ij}) + c_{ij}$, the cross term vanishes after expectation, because $\mathbb{E}[x_t - m_t^{ij}] = 0$. Hence, $\mathbb{E}[\|u_t^{ij}(x_t)\|^2] = \text{tr}(A_t^{ij} \Sigma_t^{ij} (A_t^{ij})^\top) + \|c_{ij}\|^2$. Therefore,

$$C_{ij} = \frac{1}{2} \int_0^1 \left[\text{tr}(A_t^{ij} \Sigma_t^{ij} (A_t^{ij})^\top) + \|c_{ij}\|^2 \right] dt.$$

Since $c_{ij} = m_j^1 - m_i^0$ is constant in time, this becomes

$$C_{ij} = \frac{1}{2} \|m_j^1 - m_i^0\|^2 + \frac{1}{2} \int_0^1 \text{tr} \left(A_t^{ij} \Sigma_t^{ij} (A_t^{ij})^\top \right) dt,$$

thus completing the proof. \square

References

- [ABG11] A. Arapostathis, V. S. Borkar, and M. K. Ghosh, *Ergodic Control of Diffusion Processes*, Encyclopedia of Mathematics and its Applications, Cambridge University Press, 2011, doi: <https://doi.org/10.1017/CB09781139003605>.
- [AC24] D. O. Adu and Y. Chen, *Schrödinger bridge over averaged systems*, 2024, URL: <https://arxiv.org/abs/2412.03294>.
- [AEG26] D. O. Adu, K. Elamvazhuthi, and B. Ghahesifard, *From Schrödinger bridge to optimal transport over sub-Riemannian manifolds*, 2026, URL: <https://arxiv.org/abs/2605.11429>.
- [BC09] A. Bain and D. Crisan, *Fundamentals of Stochastic Filtering*, Stochastic Modelling and Applied Probability, vol. 60, Springer, New York, 2009, doi: <https://doi.org/10.1007/978-0-387-76896-0>.
- [BHCK23] C. Bunne, Y.-P. Hsieh, M. Cuturi, and A. Krause, *The Schrödinger bridge between Gaussian measures has a closed form*, Proceedings of The 26th International Conference on Artificial Intelligence and Statistics (Francisco Ruiz, Jennifer Dy, and Jan-Willem van de Meent, eds.), Proceedings of Machine Learning Research, vol. 206, PMLR, 25–27 Apr 2023, URL: <https://proceedings.mlr.press/v206/bunne23a.html>, pp. 5802–5833.
- [Bor05] V. S. Borkar, *Controlled diffusion processes*, Probability Surveys **2** (2005), 213 – 244, doi: <https://doi.org/10.1214/154957805100000131>.
- [BTHD21] V. De Bortoli, J. Thornton, J. Heng, and A. Doucet, *Diffusion Schrödinger bridge with applications to score-based generative modeling*, Advances in Neural Information Processing Systems (held virtually), vol. 34, 2021, URL: <https://openreview.net/forum?id=9BnCwiXB0ty>, pp. 17695–17709.
- [CGP16] Y. Chen, T. T. Georgiou, and M. Pavon, *On the relation between optimal transport and Schrödinger bridges: A stochastic control viewpoint*, Journal of Optimization Theory and Applications **169** (2016), no. 2, 671–691, doi: <https://doi.org/10.1007/s10957-015-0803-z>.
- [CGP17] ———, *Optimal transport over a linear dynamical system*, IEEE Transactions on Automatic Control **62** (2017), no. 5, 2137–2152, doi: <https://doi.org/10.1109/TAC.2016.2602103>.
- [CGP18] ———, *Optimal steering of a linear stochastic system to a final probability distribution — Part III*, IEEE Transactions on Automatic Control **63** (2018), no. 9, 3112–3118, doi: [10.1109/TAC.2018.2791362](https://doi.org/10.1109/TAC.2018.2791362).
- [CGP21] ———, *Stochastic control liaisons: Richard Sinkhorn meets Gaspard Monge on a Schrödinger bridge*, SIAM Review **63** (2021), no. 2, 249–313, doi: <https://doi.org/10.1137/20M1339982>.
- [CGP25] ———, *Optimal survival strategies for diffusive flows: A Schrödinger bridge approach to unbalanced transport*, SIAM Review **67** (2025), no. 3, 579–604, doi: <https://doi.org/10.1137/25M176581X>.
- [CGT18] Y. Chen, T. T. Georgiou, and A. Tannenbaum, *Optimal transport for Gaussian mixture models*, IEEE Access **7** (2018), 6269–6278, doi: <https://doi.org/10.1109/ACCESS.2018.2889838>.
- [CH21] K. F. Caluya and A. Halder, *Wasserstein proximal algorithms for the Schrödinger bridge problem: Density control with nonlinear drift*, IEEE Transactions on Automatic Control **67** (2021), no. 3, 1163–1178, doi: <https://doi.org/10.1109/TAC.2021.3060704>.
- [CL94] P. Cattiaux and C. Léonard, *Minimization of the Kullback information of diffusion processes*, Annales de l’IHP Probabilités et statistiques, vol. 30, 1994, URL: https://www.numdam.org/item/AIHPB_1994__30_1_83_0/, pp. 83–132.
- [DD20] J. Delon and A. Desolneux, *A Wasserstein-type distance in the space of Gaussian mixture models*, SIAM Journal on Imaging Sciences **13** (2020), no. 2, 936–970, doi: <https://doi.org/10.1137/19M1301047>.
- [DE97] P. Dupuis and R. S. Ellis, *A Weak Convergence Approach to the Theory of Large Deviations*, Wiley Series in Probability and Statistics: Probability and Statistics, John Wiley & Sons, Inc., New York, 1997, doi: <https://doi.org/10.1002/9781118165904>.
- [DEDKC25] C. Domingo-Enrich, M. Drozdal, B. Karrer, and R. T. Q. Chen, *Adjoint matching: Fine-tuning flow and diffusion generative models with memoryless stochastic optimal control*, The Thirteenth International Conference on Learning Representations, 2025, doi: <https://openreview.net/forum?id=xQBRrtQM8u>.
- [DEH26] C. Domingo-Enrich and J. Han, *Adjoint matching through the lens of the stochastic maximum principle in optimal control*, 2026, URL: <https://arxiv.org/abs/2604.08580>.

- [DEHA⁺24] C. Domingo-Enrich, J. Han, B. Amos, J. Bruna, and R. T. Q. Chen, *Stochastic optimal control matching*, Advances in Neural Information Processing Systems (A. Globerson, L. Mackey, D. Belgrave, A. Fan, U. Paquet, J. Tomczak, and C. Zhang, eds.), vol. 37, Curran Associates, Inc., 2024, doi: https://proceedings.neurips.cc/paper_files/paper/2024/file/cc32ec39a5073f61d38c338d963df30d-Paper-Conference.pdf, pp. 112459–112504.
- [ECH26] A. Eldesoukey, Y. Chen, and A. Halder, *A generalized Sinkhorn algorithm for mean-field Schrödinger bridge*, 2026, URL: <https://arxiv.org/abs/2604.06531>.
- [EG25] A. Eldesoukey and T. T. Georgiou, *Schrödinger’s control and estimation paradigm with spatio-temporal distributions on graphs*, IEEE Transactions on Automatic Control **70** (2025), no. 4, 2466–2478, doi: [10.1109/TAC.2024.3485537](https://doi.org/10.1109/TAC.2024.3485537).
- [Ela26] K. Elamvazhuthi, *Flow matching for measure transport and feedback stabilization of control-affine systems*, 2026, URL: <https://arxiv.org/abs/2510.02706>.
- [EMG24] A. Eldesoukey, O. M. Miangolarra, and T. T. Georgiou, *An excursion onto Schrödinger’s bridges: Stochastic flows with spatio-temporal marginals*, IEEE Control Systems Letters **8** (2024), 1138–1143, doi: <https://doi.org/10.1109/LCSYS.2024.3409107>.
- [Föl88] H. Föllmer, *Random fields and diffusion processes*, Lecture Notes in Mathematics **1362** (1988), 101–204, doi: <https://doi.org/10.1007/BFb0086180>.
- [Fol99] G. B. Folland, *Real Analysis: Modern Techniques and their Applications*, John Wiley & Sons, 1999, URL: <https://tinyurl.com/nycd2y2y>.
- [GKBK24] N. Gushchin, S. Kholkin, E. Burnaev, and A. Korotin, *Light and optimal Schrödinger bridge matching*, Proceedings of the 41st International Conference on Machine Learning (Vienna, Austria), no. 680, JMLR.org, 2024, URL: <https://openreview.net/forum?id=EWJn6hfZ4J>, pp. 1710–17122.
- [GZZ24] J. Garg, X. Zhang, and Q. Zhou, *Soft-constrained Schrödinger bridge: a stochastic control approach*, Proceedings of the 27th International Conference on Artificial Intelligence and Statistics (AISTATS) (Valencia, Spain), vol. 238, PMLR, 2024, URL: <https://proceedings.mlr.press/v238/garg24a.html>, p. 4429–4437.
- [IK23] K. Ito and K. Kashima, *Maximum entropy optimal density control of discrete-time linear systems and Schrödinger bridges*, IEEE Transactions on Automatic Control (2023), 1536–1551, doi: <https://doi.org/10.1109/TAC.2023.3305319>.
- [KS91] I. Karatzas and S. E. Shreve, *Brownian Motion and Stochastic Calculus*, second ed., Graduate Texts in Mathematics, vol. 113, Springer-Verlag, New York, 1991, doi: <https://doi.org/10.1007/978-1-4612-0949-2>.
- [L14] C. Léonard, *A survey of the Schrödinger problem and some of its connections with optimal transport*, Discrete and Continuous Dynamical Systems **34** (2014), no. 4, 1533–1574, doi: <https://doi.org/10.3934/dcds.2014.34.1533>.
- [Lam25] M. Lambert, *The LQR-Schrödinger bridge*, 2025 IEEE 64th Conference on Decision and Control (CDC), 2025, doi: <https://doi.org/10.1109/CDC57313.2025.11312252>, pp. 3149–3156.
- [LCBH⁺23] Y. Lipman, R. T. Q. Chen, H. Ben-Hamu, M. Nickel, and M. Le, *Flow matching for generative modeling*, The Eleventh International Conference on Learning Representations, 2023, URL: <https://openreview.net/forum?id=PqvMRDCJT9t>.
- [LCST22] G.-H. Liu, T. Chen, O. So, and E. A. Theodorou, *Deep generalized Schrödinger bridge*, Advances in Neural Information Processing Systems (Louisiana, LA), vol. 35, Curran Associates, Inc., 2022, URL: <https://openreview.net/forum?id=fp33Nsh005>, pp. 9374–9388.
- [LLN⁺24] G.-H. Liu, Y. Lipman, M. Nickel, B. Karrer, E. A. Theodorou, and R. T. Q. Chen, *Generalized Schrödinger bridge matching*, International Conference on Learning Representations (Vienna, Austria), 2024, URL: <https://openreview.net/forum?id=SoismgeX7z>.
- [LS01] R. S. Liptser and A. N. Shiryaev, *Statistics of Random Processes. I. General Theory*, expanded ed., Stochastic Modelling and Applied Probability, Applications of Mathematics (New York), vol. 5, Springer-Verlag, Berlin, 2001, doi: <https://doi.org/10.1007/978-3-662-13043-8>.
- [MAJTC25] Y. Mei, M. Al-Jarrah, A. Taghvaei, and Y. Chen, *Flow matching for stochastic linear control systems*, Proceedings of the 7th Annual Learning for Dynamics & Control Conference (Necmiye Ozay, Laura Balzano, Dimitra Panagou, and Alessandro Abate, eds.), Proceedings of Machine Learning Research, vol. 283, PMLR, 04–06 Jun 2025, URL: <https://proceedings.mlr.press/v283/mei25a.html>, pp. 484–496.
- [MGM22] A. Mallasto, A. Gerolin, and H. Q. Minh, *Entropy-regularized 2-Wasserstein distance between Gaussian measures*, Information Geometry **5** (2022), no. 1, 289–323, doi: <https://doi.org/10.1007/s41884-021-00052-8>.
- [MHA26] H. Mahmood, A. Halder, and A. Akhtar, *Schrödinger bridge over a compact connected Lie group*, 2026, URL: <https://arxiv.org/abs/2603.14049>.
- [Mik21] T. Mikami, *Stochastic Optimal Transportation — Stochastic Control with Fixed Marginals*, SpringerBriefs in Mathematics, Springer, Singapore, 2021, doi: <https://doi.org/10.1007/978-981-16-1754-6>.

- [MT06] T. Mikami and M. Thieullen, *Duality theorem for the stochastic optimal control problem*, Stochastic processes and their applications **116** (2006), no. 12, 1815–1835, doi: <https://doi.org/10.1016/j.spa.2006.04.014>.
- [MT08] ———, *Optimal transportation problem by stochastic optimal control*, SIAM Journal on Control and Optimization **47** (2008), no. 3, 1127–1139, doi: <https://doi.org/10.1137/050631264>.
- [NGK26] H. Nakashima, S. Ganguly, and K. Kashima, *Globally solving unbalanced optimal transport and density control for Gaussian distributions*, 2026, URL: <https://arxiv.org/abs/2605.04246>.
- [PC20] G. Peyré and M. Cuturi, *Computational Optimal Transport*, 2020, URL: <https://arxiv.org/abs/1803.00567>.
- [Pey25] G. Peyré, *Optimal and diffusion transports in machine learning*, 2025, URL: <https://arxiv.org/abs/2512.06797>.
- [PP90] P. D. Pra and M. Pavon, *On the Markov processes of Schrödinger, the Feynman-Kac formula and stochastic control*, Realization and Modelling in System Theory: Proceedings of the International Symposium MTNS-89, Volume I, Springer, 1990, doi: https://doi.org/10.1007/978-1-4612-3462-3_55, pp. 497–504.
- [Pra91] P. D. Pra, *A stochastic control approach to reciprocal diffusion processes*, Applied Mathematics and Optimization **23** (1991), no. 1, 313–329, doi: <https://doi.org/10.1007/BF01442404>.
- [Pro04] P. E. Protter, *Stochastic Integration and Differential Equations*, second ed., Applications of Mathematics (New York), vol. 21, Springer-Verlag, Berlin, 2004, doi: <https://doi.org/10.1007/978-3-662-10061-5>.
- [RH21] L. Ruthotto and E. Haber, *An introduction to deep generative modeling*, GAMM-Mitteilungen **44** (2021), no. 2, e202100008, doi: <https://doi.org/10.1002/gamm.202100008>.
- [RPL⁺26] G. Rapakoulias, A. R. Pedram, F. Liu, L. Zhu, and P. Tsiotras, *Go with the flow: Fast diffusion for Gaussian mixture models*, Advances in Neural Information Processing Systems **38** (2026), 92879–92916, URL: <https://openreview.net/forum?id=bmznY5wYXH>.
- [RPT25] G. Rapakoulias, A. R. Pedram, and P. Tsiotras, *Steering large agent populations using mean-field Schrödinger bridges with Gaussian mixture models*, IEEE Control Systems Letters (2025), doi: <https://doi.org/10.1109/LCSYS.2025.3581859>.
- [Rud76] W. Rudin, *Principles of Mathematical Analysis*, third ed., International Series in Pure and Applied Mathematics, McGraw-Hill Book Co., New York-Auckland-Düsseldorf, 1976, doi: <https://doi.org/10.1017/S0013091500008889>.
- [RY99] D. Revuz and M. Yor, *Continuous Martingales and Brownian Motion*, third ed., Grundlehren der mathematischen Wissenschaften [Fundamental Principles of Mathematical Sciences], vol. 293, Springer-Verlag, Berlin, 1999, doi: <https://doi.org/10.1007/978-3-662-06400-9>.
- [San15] F. Santambrogio, *Optimal Transport for Applied Mathematicians: Calculus of Variations, PDEs, and Modeling*, Progress in Nonlinear Differential Equations and their Applications, vol. 87, Birkhäuser/Springer, Cham, 2015, doi: <https://doi.org/10.1007/978-3-319-20828-2>.
- [San23] ———, *A Course in the Calculus of Variations: Optimization, Regularity, and Modeling*, Universitext, Springer Nature, 2023, doi: <https://doi.org/10.1007/978-3-031-45036-5>.
- [SBCD23] Y. Shi, V. De Bortoli, A. Campbell, and A. Doucet, *Diffusion Schrödinger bridge matching*, Advances in Neural Information Processing Systems, vol. 36, Curran Associates, Inc., 2023, URL: <https://openreview.net/forum?id=qy070HsJT5>, pp. 62183–62223.
- [Sch31] E. Schrödinger, *Über die umkehrung der naturgesetze*, Sitzungsberichte der Preuss. Phys. Math. Klasse **10** (1931), 144–153, URL: <https://leonard.perso.math.cnrs.fr/papers/1931-Schroedinger-Ueber%20die%20Umkehrung%20der%20Naturgesetze.pdf>.
- [Sch32] ———, *Sur la théorie relativiste de l'électron et l'interprétation de la mécanique quantique*, Annales de l'institut Henri Poincaré **2** (1932), no. 4, 269–310 (fr), URL: https://www.numdam.org/item/AIHP_1932__2_4_269_0/.
- [SGPT26] A. Selim, S. Ganguly, A. Pakniyat, and P. Tsiotras, *Nonlinear stochastic optimal control and optimal stopping using the Fokker–Planck transformation*, 2026, URL: <https://arxiv.org/abs/2604.12153>.
- [SSDK⁺21] Y. Song, J. Sohl-Dickstein, D. P. Kingma, A. Kumar, S. Ermon, and B. Poole, *Score-based generative modeling through stochastic differential equations*, International Conference on Learning Representations (held virtually), 2021, URL: <https://openreview.net/forum?id=PxtIG12RRHS>.
- [TMF⁺23] A. Tong, N. Malkin, K. Fatras, L. Atanackovic, Y. Zhang, G. Huguet, G. Wolf, and Y. Bengio, *Simulation-free Schrödinger bridges via score and flow matching*, Proceedings of the 27th International Conference on Artificial Intelligence and Statistics (AISTATS) 2024, Valencia, Spain. **238** (2023), URL: <https://doi.org/10.48550/arXiv.2307.03672>.
- [TWH26] A. M. H. Teter, W. Wang, and A. Halder, *Schrödinger bridge with quadratic state cost is exactly solvable*, IEEE Transactions on Automatic Control **71** (2026), no. 5, 2903–2917, doi: <https://doi.org/10.1109/TAC.2025.3631521>.
- [Vil03] C. Villani, *Topics in Optimal Transportation*, Graduate Studies in Mathematics, vol. 58, American Mathematical Society, Providence, RI, 2003, doi: <https://doi.org/10.1090/gsm/058>.

- [YZ99] J. Yong and X. Y. Zhou, *Stochastic Controls: Hamiltonian Systems and HJB Equations*, Applications of Mathematics (New York), vol. 43, Springer-Verlag, New York, 1999, doi: <https://doi.org/10.1007/978-1-4612-1466-3>.